01
April 2020
Volume 2 Issue 1

Journal of Marine Science

BILINGUAL PUBLISHING CO.
Pioneer of Global Academics Since 1984

APSCI | creative commons | CNKI 中国知网 www.cnki.net 中国知识基础设施工程
Google scholar | Crossref | MyScienceWork

Volume 2 | Issue 1 | April 2020 | ISSN 2661-3239 (Online)

ISSN 2661-3239 01
9 772661 323200

Volume 2 Issue 1 • April 2020 • ISSN 2661-3239 (Online)

Journal of Marine Science

BILINGUAL PUBLISHING CO.
Pioneer of Global Academics Since 1984

BILINGUAL PUBLISHING CO.
Pioneer of Global Academics Since 1984

Volume 2 | Issue 1 | April 2020 | Page 1-37
Journal of Marine Science

Contents

Article

Review

BILINGUAL PUBLISHING CO.
Pioneer of Global Academics Since 1984

Journal of Marine Science
http://ojs.bilpublishing.com/index.php/jms

ARTICLE

Aluminium Induced DNA-damage and Oxidative Stress in Cultures of the Marine Sponge *Hymeniacidon perlevis*

Rachael Ununuma Akpiri[1] Rosline Sonayee Konya[2] Nikolas John Hodges[1*]

1. School of Biosciences, University of Birmingham, United Kingdom
2. Department of Animal and Environmental Biology, University of Port Harcourt, Nigeria

ARTICLE INFO

Article history
Received: 24 July 2019
Accepted: 19 September 2019
Published Online: 29 December 2019

Keywords:
Aluminium
Comet assay
DNA Damage
ROS
Sponge
Hymeniacidon perlevis

ABSTRACT

Aluminium is the most abundant element in the earth crust and has no known biological function. However, it is an established neurotoxicant in its trivalent oxidation state, with exposure resulting in neurodegenerative diseases like Parkinson's disease and presenile dementia. Although the potential genotoxic and carcinogenic effects of aluminium are established in mammalian and other model systems, there is however very limited information on aluminium genotoxicity in aquatic invertebrates. Mechanism of aluminium toxicity is also largely unclear. With a concentration range between 0.001– 0.05mg/L in near-neutral pH water, and up to 0.5-1mg/L in acidic water , aluminium poses a potential threat to the marine ecosystem, however, it is poorly studied. This study therefore presents for the first time, aluminium-induced DNA damage using the comet assay and Reactive Oxygen Species (ROS) formation using 2', 7'-dichlorodihydrofluorescein diacetate (H2DCF-DA) assay as biomarkers of genotoxicity and oxidative stress in the inter-tidal marine sponge *Hymeniacidon perlevis*, respectively. *H. perlevis* is widely distributed in the British Isles, Mediterranean and the Arctic sea and has been reported as a model for environmental biomonitoring in aquatic ecosystem and as a suitable alternative to bivalves. In this study, cryopreserved single sponge cells of *H. perlevis* were cultured as viable aggregates and were thereafter treated with 0.1, 0.2, 0.3 and 0.4mg/L aluminium chloride (AlCl3) for 12 hours. Cell viability was determined using the 3-(4,5-dimethylthiazol-2-yl)-2,5-diphenyltetrazolium bromide (MTT) assay. Our results showed that non-cytotoxic concentrations of AlCl3 caused a statistically significant concentration-dependent increase in the level of DNA-strand break and reactive oxygen species formation single sponge cells of *H. perlevis*. There was also a statistically significant positive linear correlation between aluminium-induced DNA strand break and ROS formation suggesting the involvement of ROS in the causative mechanism of the aluminium induced DNA-strand breaks observed.

1. Introduction

Marine sponges are simple invertebrate animals with ecological importance in the aquatic ecosystem. A prominent feature of sponges that have advanced their ecological usefulness is their ability to pump large volumes of water through their body tissues during filter feeding. During this process, large amounts of particulate matter both in their dissolved and suspended phase, including xenobiotics are trapped within the

**Corresponding Author:*
Nikolas John Hodges,
School of Biosciences, University of Birmingham, United Kingdom;
Email: n.hodges@bham.ac.uk

 DOI: https://doi.org/10.30564/jms.v2i1.1070

sponge tissues[1,2]. These materials are mostly retained within the animal and constitute vital sources of information for biomonitoring and risk assessment of their immediate aquatic ecosystem. *Hymeniacidon. perlevis*, a demosponge belonging to the order suberitida, family halochondridae and genus *Hymeniacidon* is a commonly utilised sponge species for biomonitoring, bioremediation, bioactive compound analysis and water quality [3-6]. It is an intertidal species widely distributed on the British Isles, Mediterranean and the Arctic sea; with records of appearance in Belgium and France. Depending on exposure, *H. perlevis* assumes different colours ranging from very bright orange to blood red and sometimes yellowish-orange to pinkish-red (Figure 1). *H. perlevis* has a well-defined seasonal life cycle with four developmental stages; dormancy, resuscitation, bloom and decline stages which are useful for predicting environmental changes. Current sponge research is focused on the development and maintenance in a culture of functional sponge aggregates (primorphs), which is thought to be the future for sustainable production of sponge bioactive metabolites, investigation of response to environmental chemical exposure in the aquatic ecosystem, and genomic annotations [8-11]. Previous studies comparing *H. perlevis* with its counterpart sentinel bivalve neighbour; *Mytilus. edulis* (the blue mussel) as models for environmental biomonitoring, shows that *H. perlevis* accumulates certain in-situ pollutants up to 10-fold more [4]. Also, *Hymeniacidon* has been reported to be more sensitive in the detection of petrogenic and pyrogenic xenobiotics than the brown mussel: *P. perna* [7]. Several studies have utilised H. perlevis as a model for the investigation of important biochemical processes and chemical exposure. Recently, DNA damage induction following exposure of *H. perlevis* cells to environmentally relevant concentrations of Cadmium, Chromium, Nickel and Benzo[a] Pyrene showed a concentration-dependent increase in DNA damage [6,12] which is consistent with the findings in this present study. Hence, H. perlevis , therefore, is a suitable species for environmental risk assessment and biomonitoring pollutants in the aquatic medium and it is reliable sentinel representative for investigating the impact of environmental stressors on aquatic biota.

Among pollutants accumulated by sponges, heavy metals and organic pollutants have been extensively studied [2,12-16]. Heavy metals bioaccumulation in sponges are reported even when concentrations are very low and below the limit of detection in other environmental samples such as surrounding water and sediments [7,17-19]. Ferrante, Vassallo [1] have also demonstrated the potential of sea sponge to bioaccumulate a wide range of organic pollutants both *in vitro* and *in situ*. There is, however, limited information on the biological effects of aquatic pollutants and their biomarkers in marine sponges which are needed if these species are to be developed as reliable tools for risk assessment and biomonitoring. One such reliable biomarker of effect and exposure to environmental pollutants in both humans and animals is DNA damage and it has been widely applied in assessing the biological effects of environmental pollutants in established model systems [20-22]. Although the genotoxic potential of pollutants in marine sponges has been demonstrated previously [6,12,23] much less is known compared to other species and there is no information on the genotoxic effects of emerging pollutants like aluminium to these potentially important organisms.

The toxicity and mechanism of toxicity of most class B and borderline heavy metals (Cd, Cr, Cu, Ni, Pb, Hg, Co, Ag, Au,) are well established as is their deleterious effects on human health and involvement in the pathology of diseases including cancer [24-26]. In contrast, class A metals (Al, Be, Li, Ca, K etc) are often considered as essential metals with a strong affinity for oxygen [27,28], and were considered until recently as relatively non-toxic or having very low potential to exert adverse health effects [29]. Aluminium, for example, is the third most abundant element and the most abundant metal in the earth crust, making up to 8% of the earth crust and occurs as oxides, hydroxides or silicates of sodium or fluorides and as organic matter complexes with wide industrial application [29,30]. Major uses and applications are in construction companies, aircraft production, and automobile industries and as alloys [29]. However, some reports that have shown the toxic potential of aluminium in both humans and animals. Iron-induced reactive oxygen species formation and lipid peroxidation, protein phosphorylation, apoptosis, and interference with gene expression, have all been reported following exposure to aluminium [31-33]. Other studies have also demonstrated chromosome aberrations, induction of micronuclei, and sister chromatid exchange induced by aluminium exposure [31,34]. Furthermore, the involvement of aluminium in the aetiology of neurodegenerative disorders such as presenile Alzheimer's and Parkinson's disease has also been reported and studied [35]. Therefore, there are potential genotoxic and carcinogenic effects of aluminium [31,33,36,37], however, the mechanism of aluminium genotoxic and carcinogenic pathways remain largely unclear [31]. In the marine environment aluminium concentration in water varies depending on pH, for example, ranges such as 0.001– 0.05mg/L were recorded in near-neutral pH water while up to 0.5-1mg/L was recorded in acidic water [29] making it a potential but poorly studied threat to the marine environment. This study presents for the first time,

DOI: https://doi.org/10.30564/jms.v2i1.1070

aluminium-induced DNA damage and reactive oxygen Species (ROS) formation in cultured sponge cells exposed to non-cytotoxic concentrations of aluminium.

2. Materials and Methods

2.1 Sponge Collection and Preservation

Samples of the marine sponge *H perlevis* were collected from Tenby Bay castle beach in Pembrokeshire, South Wales, UK on exposed rock pools at low tide. These were immediately transported back to the laboratory in aerated seawater and processed into single cells and thereafter cryopreserved in vapour phase liquid nitrogen following a previously described protocol with modifications [38]. Briefly, single sponge cells were isolated from sponge tissues using ethylene diamine tetra acetic acid (EDTA) containing calcium magnesium-free seawater (CMFSW+E) and calcium magnesium-free seawater (CMFSW) prepared according to Cold Spring Harbor Laboratory Protocols [39]. CMFSW-E (450 mM NaCl, 9 mM KCl, 37 mM Na_2SO_4, 2.2 mM $NaHCO_3$, 10 mM Tris-HCl pH 8.0, 20 mM Na_2EDTA) and CMFSW (450 mM NaCl, 9 mM KCl, 37 mM Na_2SO_4, 2.2 mM $NaHCO_3$, 10 mM Tris-HCL pH 8.0).

Freshly collected sponge samples were carefully cleaned to remove debris and dirt, washed three times in filtered natural seawater and chopped into cubes approximately $1cm^3$ with a sterile scalpel. Sponge cubes were transferred into 50 mL falcon tubes containing 40 mL CMFSW+E at a ratio of 1:5 (sponge tissue to CMFSW+E) and then placed on a rotor shaker (Rotator Labnet Orbit 1900). Tubes were allowed to shake gently at 40 rpm, first for 20 minutes at room temperature and then 60 minutes after discarding the initial CMFSW+E solution and refilling with fresh 40 mL solution. Using a 250 µm nylon mesh, single sponge cells were collected by filtering the CMFSW+E soaked tissues into a 50 mL falcon tube and pellets obtained at 300 x g for 7 minutes and the supernatant discarded.

The resulting single sponge cell pellets were then washed three times with CMFSW and resuspended in 1mL freezing media made of sponge media (made from 16.5 g instant ocean sea salt in 500 ml Ultra High Quality water - according the manufacturers instruction described at http://www.instantocean.com), 0.2% RPMI (Roswell Park Memorial Institute medium), 1mg/mL PSG (penicillin, streptomycin, glutamine) solution, 0.1% v/v Pluronic® F-68, 10% v/v DMSO-dimethylsulfoxide (cryoprotectant), and 10% FBS (Foetal bovine serum). 1 mL freezing re-suspended single cells were then aliquoted into corning cryogenic vial and stored overnight in a -80^0C freezer before been transferred to vapour phase liquid Nitrogen for long term storage until required.

2.2 Sponge Cell Culture and Aggregate Formation

Cryopreserved sponge cells were quickly thawed in a water bath at 37^oC and re-suspended in 5.5 mL sponge media; sponge cell pellets were obtained by centrifuging cell suspension for 7 minutes at 300 x g. Pellets were then resuspended in 6 mL and cell density and viability determined using a haemocytometer (Neubauer improved superior Marienfield, Germany) and trypan blue staining. For sponge cell culture, approximately, 20 x 10^6 cells/mL were placed in sterile T_{25} culture flasks and made up to a final volume of 6 mL with sponge media and left on a horizontal rotator shaker at 45 rpm at room temperature for up to 12 hours. The culture media was changed daily for the first three days, allowing aggregates to settle under gravity for approximately 5 minutes before carefully taking out 3 mL of the media and replacing with 3 mL of fresh media. Sponge cells rapidly formed aggregates that maintained viability for more than 1 week in culture (as shown by MTT viability assay: data not shown).

2.3 'In vivo' Exposure Sponge Cell Model

In a minimum of three independent experimental repeats, aggregates were exposed to 0 mg/L, 0.1 mg/L, 0.2m/L, 0.3 mg/L and 0.4 mg/L aluminium chloride for 12 hours. All experiments were conducted at room temperature in 12-well cell culture cluster flat bottom with lid plate (Corning) placed on a horizontal shaker set at 45 rpm.

2.4 3-(4, 5-dimethylethiazole-2-yl)-2,7-diphenyl-etetrazoliumbromide (MTT) Viability Assay

Following 12 hours laboratory exposures of *H perlevis* sponge cell aggregates to different concentrations of aluminium chloride, MTT viability assay was performed to investigate potential cytotoxic effects of the test concentrations on sponge cell aggregates. Dissociated single sponge pellets were washed 3 x 5mL with CMFSW (to remove the EDTA) and then re-suspended in 1mL 0.5 mg/mL MTT in sponge media. All cell suspensions were then transferred into 6 well plates and incubated at 37^oC for three hours. After incubation, well plate contents were transferred into Eppendorf tubes and centrifuged again at the same speed and time as before and the resulting pellets were suspended in 100 µL DMSO. MTT reduction of the DMSO solubilized cells was then visualized at 570 nm absorption with infinite 200 Pro spectrophotometer against a 100 µl DMSO blank in 96 well corning transparent flat bottom plates.

 DOI: https://doi.org/10.30564/jms.v2i1.1070

2.5 Comet Assay Procedure for the Assessment of DNA Strand Breaks

Briefly, aluminum treated sponge cell aggregates were dissociated into single cell and the suspensions pelleted on a bench top Sanyo Gallen Kemp Micro centaur centrifuge at 8000 rpm for 7 minutes; supernatants were discarded and pellets re-suspended in 100µL CMFSW without EDTA. 15 µL of CMFSW suspended cells aliquots (in duplicates) were mixed with 150 µL of 0.5% w/v molten low melting point agarose (LMPA) in PBS and added to previously coated microscope slides (with 0.5% w/v normal melting point agarose in phosphate buffered saline (PBS). These were covered with cover slips and placed on a cold metal block for a minimum of 20 minutes to allow the gel to set.

After 20 minutes cover slips were gently slide off horizontally and slides transferred into previously chilled lysis buffer (made from 2.5 M NaCl, 100 mM EDTA, 1% sodium N-lauryl sarcosinate, 10% dimethylsulfoxide, 1% Triton X-100, 10 mM Tris, adjusted to pH 10.0) in a Coplin jar and incubated for 1 hour. Afterwards, slides were transferred into a horizontal electrophoresis tank model: GSA/VA FisherBiotech™ Horizontal Electrophoresis Systems, containing electrophoresis buffer (80 mL 9 M NaOH, and 12 mL 200 mM EDTA, and made up to a final volume of 2400 mL with UHQ water, pH ≥13.0). An unwinding time of 45 minutes was allowed without any power, next 300 mA current at a voltage of 32V was applied to the electrophoresis setup for 30 minutes. Following electrophoresis, slides were washed 3x with 5mL neutralization buffer (0.4M Tris base in 500mL UHQ water, pH 7.5) and then stained with 50 µL sybr gold (Invitrogen) fluorescent dye (1 µL in 1000 µL neutralization buffer) and cover slipped. Slides were then left in a moist box in the dark in the cold room overnight. Images were visualized with fluorescent microscope using x40 oil immersion objective and analysed with comet IV software. Statistically analysed median value of the percentage-mean-tail-intensity of 50 comet scores per slides were utilised as the genotoxicity end point [40].

2.6 DCFH-DA Assay for the Measurement of Reactive Oxygen Species (ROS)

To measure the fluorescent intensity of DCF proportional to the amount of ROS produced as a biomarker of oxidative stress induction from aluminium exposure, 100 µL of aluminium chloride treated single sponge cell suspension (obtained as in the comet assay procedure) was mixed with 1 mL aliquot of 3 µL 100 µM 2',7'-dichlorodihydrofluorescein diacetate (H_2DCFDA) and 1 mL RPMI mixture in 6 well plate. Plate was wrapped in aluminium foil to protect from light and incubated at room temperature on the bench, after 1 hour incubation, sponge cells were digested in 100 µL of 10 mM NaOH and pelleted on a bench top centrifuge at 8000 rpm for 5 minutes; supernatants were carefully aliquoted into 96 well plates and fluorescence measured at 485 nm excitation, 535 nm emissions and 10 nm band width with 200 pro infinite spectrometer.

2.7 Statistical Analysis

Results were analysed in duplicates in three technical repeats for all experiments. Using IBM SPSS version 22.0 and Graph pad prism version 7.0.2. All data were checked for normality and homogeneity of variance using Shapiro Wilk's test and Leven's test respectively. Differences between control measurements and test concentrations for all data were analysed using 1way ANOVA and Bonferroni multiple comparison Post Hoc test, at P= 0.05. Comparison between DNA damage and reactive oxygen species formation was evaluated with Pearson correlation coefficient.

3. Results

3.1 Sponge Cell Culture and Viability Assessment

Cryopreserved single sponge cells rapidly formed viable aggregates in cultures (Figure 2). Following treatments with $AlCl_3$ (0.1mg/L, 0.2mg/L, 0.3mg/L and 0.4mg/L) for 12 hours aggregates were assessed for viability using the MTT assay. The results obtained showed that the Al concentrations used in this study do not have any significant cytotoxic effect on *H. perlevis* aggregates (Figure 3). As a positive control, aggregates were also treated with known cytotoxic concentration of cadmium chloride, sodium dichromate and nickel chloride (Figure 4). Furthermore, concentrations of $AlCl_3$ up to 100µM (2.7mg/L) were also shown to be non-cytotoxic as assessed by the MTT assay (data not shown).

3.2 Aluminium-induced DNA Strand Breaks

Induction of DNA-strand breaks was assessed using the comet assay in sponge aggregates treated with non-cytotoxic concentrations of $AlCl_3$. Untreated sponge nucleoids were spherical with no evidence of DNA comets (Figure 5A), in contrast, following treatment with $AlCl_3$ clear comet tails were apparent (Figure 5B) and there was a concentration-dependent (1-Way ANOVA with Dunnett's multiple comparison tests, $P < 0.05$) increase in the levels of DNA-strand breaks as quantified by tail DNA % (Figure 5C). Mean ± SEM values of percentage median tail intensities, were 1.8 ± 0.5 (control/untreated samples), 4.9 ± 0.9 (0.1mg/L treatment), 9.0 ± 1.6 (0.2mg/l), 14.9 ± 2.7 (0.3mg/L) and 23.1 ± 3.6 (0.4mg/L treatment).

DOI: https://doi.org/10.30564/jms.v2i1.1070

3.3 Aluminium Induced Reactive Oxygen Species Correlates with DNA-strand Breaks

ROS formation as assessed by oxidation of DCF-DA following aluminium exposure was also statistically significant at $P^{*} < 0.05$ and $P^{****} < 0.0001$ (Figure 6) and concentration-dependent. DCF-Fluorescence intensity measurements following the 12 hours Aluminium exposures were expressed as Mean fluorescence intensities ± Standard error of Mean; n =3, for control, 0.1, 0.2, 0.3, and 0.4 as 20410 ± 2956, 53776 ± 10960, 61308 ± 12071, 118495 ± 11088 and 136220 ± 4874. Furthermore, DNA strand breaks and levels of reactive oxygen species positively correlated (Figure 7).

4. Discussion

The toxicity of aluminium is largely associated with its solubility in water in an acidic pH, while aluminium in neutral pH is generally thought to be insoluble, non-bioavailable and thus, less toxic [30]. This study presents for the first time the application of the alkaline comet and H2DCF-DA assays to assess aluminium-induced DNA strand breaks and reactive oxygen species (ROS) formation in laboratory cultures of marine sponge cell aggregates, as biomarkers of effects and exposure to aluminium chloride. In the current study cryopreserved single sponge cells were cultured in synthetic seawater and consistent with previous work [6] rapidly formed viable aggregates that proved a useful "*in vivo*" exposure model that was also could be readily dissociated into single-cell suspension using calcium magnesium-free seawater containing EDTA for down-stream biochemical and toxicological investigations.

The comet assay's sensitivity among other advantages distinguishes it from other in vitro genotoxicity assays and it is widely employed in environmental risk assessment of model environmental pollutants in both humans and animals [21,31]. The alkaline comet assay detects alkaline labile sites and double and single-stranded DNA breaks induced by genotoxic agents [41,42]. Previous studies have demonstrated the mutagenic and genotoxic potential of aluminium in mammalian cells using assays such as micronucleus assay, Ames test, and sister chromatid exchange assay [43-45] but there is limited data on aluminium genotoxicity in marine species. In the current study using our novel *in vivo* exposure model, non-cytotoxic concentrations of aluminium caused a concentration-dependent increase in DNA strand breaks. This is similar to the report of [46]; strains of *Salvelinus fontinalis* (Brook trout) kept in a mimicked '*in situ* field exposure' condition showed greater sensitivity to the combined toxic effect of low pH and aluminium than free-swimming ones. Significant reduction in survival rate and fish weight was observed following exposure to aluminium concentration between 29 µg/L and 222 µg/L at pH less than 4.8. Although the concentrations used in the current study were relatively high, the toxic effects of aluminium observed suggests a potential for toxic effects following chronic exposure of sponges to lower concentrations. In addition, solid aluminium particles like other metals in the aquatic system are biologically available through cellular uptake pathways [47, 48] which are enhanced by increase aluminium levels in some marine environment and may result in high local intracellular concentrations.

In the aquatic environment, aluminium accumulates in invertebrates' body tissues and the gills of gill breathing animals with toxicity being directly linked with high concentration from acidification [49-52]. According to the report of Ingersoll, Gulley [46] however, more pronounced toxicity were observed in the gills of two strains of *Salvelinus fontinalis* (Brook trout) exposed to low pH and elevated aluminium than those exposed to only low pH. Although not widely considered an environmental pollutant, aluminium concentrations as high as 9560-25000mg/kg in sediment [53]; 1830-2170µg/g in water [54] and 222.2–662.6µg/g in marine sponge tissues taken from the Niger Delta environment (Akpiri et al., in draft). Aluminium toxicity in aquatic invertebrates has been previously reported. For example, sub-lethal toxicity of aluminium has been investigated in the freshwater crustacean crayfish: *Pacifastacus leniusculus*. Marked behavioural dysfunction was observed following exposure to 500µg/L of freshly neutralised aluminium for 5 days with over 70% aluminium accumulation mainly in the gills rather than the body [30]. Exley, Wicks [32] and Kádár, Salánki [55] have also demonstrated aluminium toxicity in fish and benthic mollusc. However, to the best of our knowledge, this is the first report on the toxicity of aluminium in marine sponges. There is no known biological function of aluminium; however, in humans, the involvement of aluminium in neurodegenerative disorders such as Alzheimer's disease and Parkinson's disease has been reported [24,56].

The mechanism of metal-induced DNA damage is often linked to the production of reactive oxygen species radicals [24,57]. For example, transition metals undergo redox cycling and are able to deplete levels of intracellular glutathione which results in the production of reactive oxygen radicals (H_2O_2, $O_2^{\cdot-}$, $OH^{\cdot}$, $^1O_2$), induction of lipid peroxides and oxidative DNA damage. To investigate the involvement of reactive oxygen species involvement in aluminium genotoxicity, we measured the amount of ROS produced following treatment with $AlCl_3$ and observed a concentration-dependent increase in levels of ROS following treatment. Similar induction of ROS following aluminium exposure has been previously reported in male

 DOI: https://doi.org/10.30564/jms.v2i1.1070

rabbit [33,36]. Our data is the first on aluminium-induced reactive oxygen species in marine sponges and aluminium mediated oxidative stress in aquatic invertebrates. The results obtained demonstrated a statistically significant correlation (R^2 = 0.9974) between DNA damage and reactive oxygen species formation.

We conclude that Al is genotoxic even at non-cytotoxic concentrations with active induction of oxidative stress. The strong correlation observed between Aluminium induced oxidative DNA damage and reactive oxygen species formation, suggests the active involvement of reactive oxygen radicals in the mechanism of aluminium mediated toxicity in this experimental model. Further studies are required to reassess the potential toxicity of aluminium and the involvement of other biomarkers in the mechanistic pathways in the marine environment.

Appendixes

List of Figures

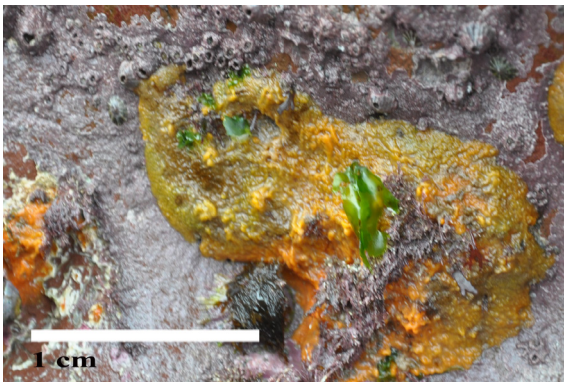

Figure 1. *Hymeniacidon* perlevis *in situ* on an exposed boulder at low tide in Tenby Bay Castle beach, Pembrokeshire

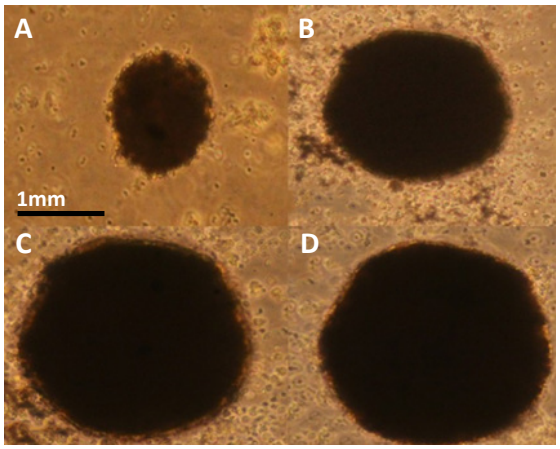

Figure 2. Representative examples of sponge cell aggregates formation after: A) 24hrs, B) 48hrs, C) 72hrs and D) 7 days in culture

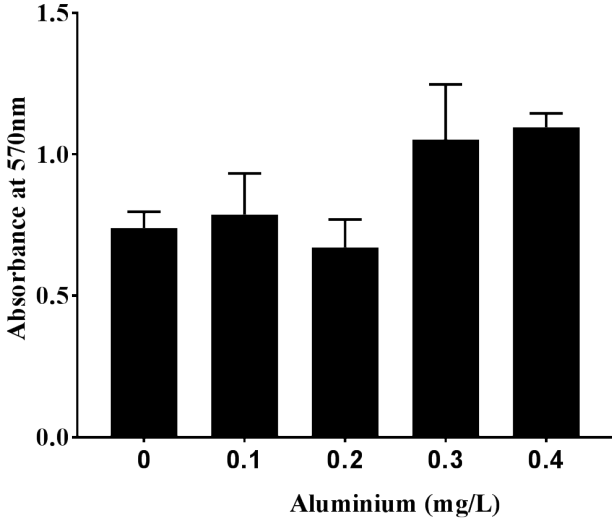

Figure 3. MTT viability assay of sponge cell aggregates exposed 12- hours in Aluminium III Chloride solution (0, 0.1, 0.2, 0.3 and 0.4mg/L)

Note: Data represent mean absorbance at 570 ± SEM, n =3. In all Aluminium exposures there was no cytotoxic effect on sponge cells by 1-Way ANOVA using Graph pad Prison version 7, P < 0.05

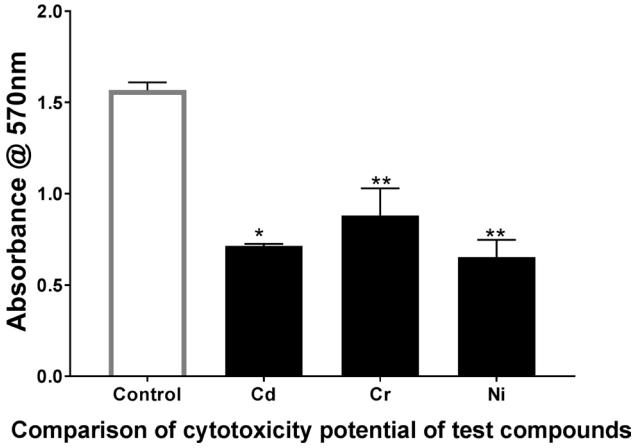

Figure 4. MTT viability assessment of positive control treatments with 100µM, Cd, Cr and Ni

Note: Mean absorbance ±SEM, n=3; P < 0.05 are presented. Results of 1-way ANOVA with Dunett's multiple comparison test, analysed with Graph pad prison 7.03 shows a statistically significant difference between the absorbance of control and treated sponge cell aggregates, * P<0.05 and ** P<0.01 respectively.

DOI: https://doi.org/10.30564/jms.v2i1.1070

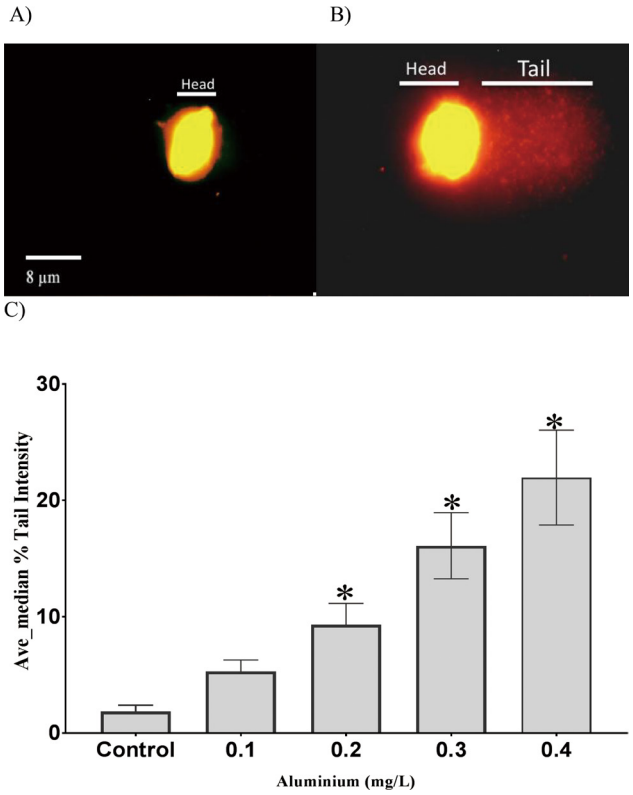

Figure 5. Representative comets images of sponge comet nucleoids, A) control B) 0.3mg/L $AlCl_3$. C) DNA strand breaks in sponge cell aggregate cultures expressed as % DNA tail intensity, following treatment with 0–0.4 mg/L aluminium chloride for 12 hours.

Note: Displayed data shows Mean values ± SEM, n= 3, $P^{**} < 0.05$ 1 way ANOVA, Shapiro Wilk's test of normality $P^{*} < 0.05$. Result shows statistically significant concentration-dependent increase in the level of DNA strand breaks from control samples.

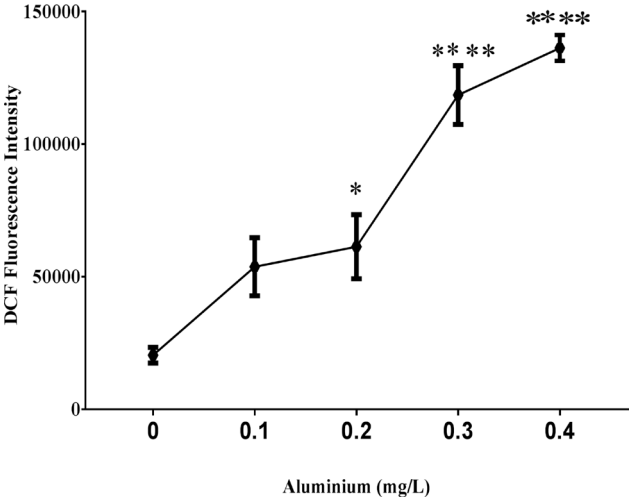

Figure 6. Aluminium Induced Oxidative stress in cultures of sponge cell aggregates

Note: Amount of reactive Oxygen Species formed increased with Increasing aluminium concentration. Data displayed are Mean values ± SEM, n = 3; statistically significant increase in DCF-fluorescence at P*<0.05 and P****<0.0001 was analysed using 1-way ANOVA with Bonferroni correction multiple comparison post-hoc test on Graph pad prison 7.0, Results represent triplicate exposures in three repeat experiments. Test of homogeneity of variance and normality performed with Levene's test and Shapiro Wilk's test using IBM SPSS.

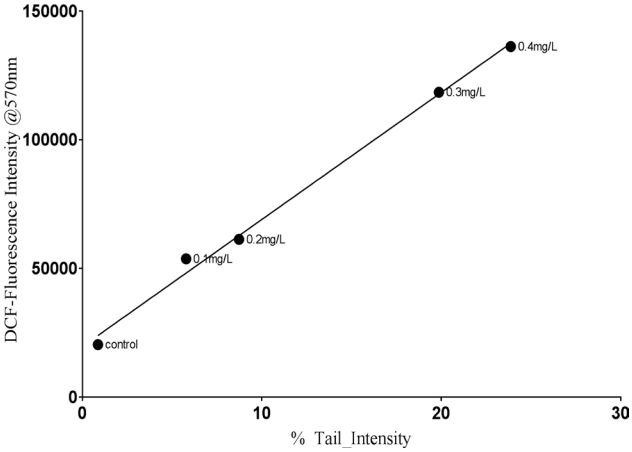

Figure 7. Correlation analysis of DCF- Fluorescent intensity versus Median % Tail Intensity in sponge cell aggregates exposed to 0, 0.2, 0.3 and 0.4mg/L aluminium chloride for 12 hours

Note: Result showed very significant correlation between ROS formation and DNA strand breaks in aluminium treated Sponge aggregates. $R^2 = 0.9974$.

References

[1] Ferrante, M., et al.. *In vivo* exposure of the marine sponge Chondrilla nucula Schmidt, 1862 to cadmium (Cd), copper (Cu) and lead (Pb) and its potential use for bioremediation purposes. Chemosphere, 2018, 193: 1049-1057.

[2] Cebrian, E., M.J. Uriz, and X. Turon. Sponges as biomonitors of heavy metals in spatial and temporal surveys in northwestern Mediterranean: multispecies comparison. Environmental Toxicology and Chemistry, 2007, 26(11): 2430-2439.

[3] Zheng, L., et al.. Identification of norharman as the cytotoxic compound produced by the sponge (*Hymeniacidon* perleve)-associated marine bacterium Pseudoalteromonas piscicida and its apoptotic effect on cancer cells. Biotechnology and applied biochemistry, 2006, 44(3): 135-142.

[4] Mahaut, M.-L., et al.. The porifera *Hymeniacidon* perlevis (Montagu, 1818) as a bioindicator for water quality monitoring. Environmental Science and Pollution Research, 2013, 20(5): 2984-2992.

[5] Longo, C., et al.. Bacterial accumulation by the Demospongiae *Hymeniacidon* perlevis: a tool for the bioremediation of polluted seawater. Marine pollution bulletin, 2010, 60(8): 1182-1187.

[6] Akpiri, R.U., R.S. Konya, and N.J. Hodges. Devel-

opment of cultures of the marine sponge *Hymeniacidon* perleve for genotoxicity assessment using the alkaline comet assay. Environmental toxicology and chemistry, 2017.

[7] Batista, D., et al.. Marine sponges as bioindicators of oil and combustion derived PAH in coastal waters. Marine environmental research, 2013, 92: 234-243.

[8] Cai, X., et al.. Establishing primary cell cultures from Branchiostoma belcheri Japanese. In Vitro Cellular & Developmental Biology-Animal, 2013, 49(2): p. 97-102.

[9] Pomponi, S.A., R. Willoughby. Development of sponge cell cultures for biomedical application, 2000.

[10] Pomponi, S., R. Willoughby. Sponge cell culture for production of bioactive metabolites. Sponges in time and space. Balkema, Rotterdam, 1994: 395-400.

[11] de Caralt, S., M.J. Uriz, R.H. Wijffels. Cell culture from sponges: pluripotency and immortality. Trends in biotechnology, 2007, 25(10): 467-471.

[12] Schröder, H.C., et al.. Stress response in Baikalian sponges exposed to pollutants. Hydrobiologia, 2006, 568: 277-287.

[13] Perez, T., et al.. Marine sponges as biomonitor of polychlorobiphenyl contamination: concentration and fate of 24 congeners. Environmental science & technology, 2003. 37(10): 2152-2158.

[14] Zahn, R., et al.. The effect of benzo [a] pyrene on sponges as model organisms in marine pollution. Chemico-biological interactions, 1982, 39(2): 205-220.

[15] Pan, K., et al.. Sponges and sediments as monitoring tools of metal contamination in the eastern coast of the Red Sea, Saudi Arabia. Mar Pollut Bull, 2011, 62(5): 1140-6.

[16] Rao, J.V., et al.. Environmental contamination using accumulation of metals in marine sponge, Sigmadocia fibulata inhabiting the coastal waters of Gulf of Mannar, India. Toxicological & Environmental Chemistry, 2007, 89(3): 487-498.

[17] Hill, M., et al.. Toxic effects of endocrine disrupters on freshwater sponges: common developmental abnormalities. Environmental Pollution, 2002, 117(2): 295-300.

[18] Olesen, T. and J. Weeks, Accumulation of Cd by the marine sponge Halichondria panicea Pallas: effects upon filtration rate and its relevance for biomonitoring. Bulletin of environmental contamination and toxicology, 1994, 52(5): 722-728.

[19] Hansen, I.V., J.M. Weeks, and M.H. Depledge, Accumulation of copper, zinc, cadmium and chromium by the marine sponge Halichondria panicea Pallas and the implications for biomonitoring. Marine Pollution Bulletin, 1995, 31(1-3): 133-138.

[20] Ahmed, M., et al.. Chromium (VI) induced acute toxicity and genotoxicity in freshwater stinging catfish, Heteropneustes fossilis. Ecotoxicology and environmental safety, 2013, 92: 64-70.

[21] Martins, M. P.M. Costa. The comet assay in environmental risk assessment of marine pollutants: applications, assets and handicaps of surveying genotoxicity in non-model organisms. Mutagenesis, 2014, 30(1): 89-106.

[22] Sarkar, A., et al.. Genotoxicity of cadmium chloride in the marine gastropod Nerita chamaeleon using comet assay and alkaline unwinding assay. Environmental toxicology, 2015, 30(2): 177-187.

[23] Schröder, H.C., et al.. Induction of DNA strand breaks and expression of HSP70 and GRP78 homolog by cadmium in the marine sponge Suberites domuncula. Arch Environ Contam Toxicol, 1999, 36(1): 47-55.

[24] Stohs, S.J. D. Bagchi. Oxidative mechanisms in the toxicity of metal ions. Free radical biology and medicine, 1995, 18(2): 321-336.

[25] Henkler, F., J. Brinkmann, A. Luch. The role of oxidative stress in carcinogenesis induced by metals and xenobiotics. Cancers, 2010, 2(2): 376-396.

[26] IARC, IARC Monographs on the Evaluation of Carcinogenic Risks to Humans: Chromium, Nickel and Welding. IARC Working Group on the Evaluation of Carcinogenic Risks to Humans. 1990: International Agency for Research on Cancer.

[27] Deb, S., T. Fukushima. Metals in aquatic ecosystems: mechanisms of uptake, accumulation and release-Ecotoxicological perspectives. International Journal of Environmental Studies, 1999, 56(3): 385-417.

[28] Rainbow, P.S., The biology of heavy metals in the sea. International Journal of Environmental Studies, 1985, 25(3): 195-211.

[29] Krewski, D., et al., Human health risk assessment for aluminium, aluminium oxide, and aluminium hydroxide. Journal of Toxicology and Environmental Health, Part B, 2007, 10(S1): 1-269.

[30] Alexopoulos, E., et al.. Bioavailability and toxicity of freshly neutralized aluminium to the freshwater crayfish *Pacifastacus leniusculus*. Archives of Environmental Contamination and Toxicology, 2003, 45(4): 509-514.

[31] Lankoff, A., et al.. A comet assay study reveals that aluminium induces DNA damage and inhibits the repair of radiation-induced lesions in human peripheral blood lymphocytes. Toxicology letters, 2006. 161(1): 27-36.

[32] Exley, C., et al.. Kinetic constraints in acute alumin-

DOI: https://doi.org/10.30564/jms.v2i1.1070

ium toxicity in the rainbow trout (Oncorhynchus mykiss). Journal of theoretical biology, 1996, 179(1): 25-31.

[33] Yousef, M.I., Aluminium-induced changes in hemato-biochemical parameters, lipid peroxidation and enzyme activities of male rabbits: protective role of ascorbic acid. Toxicology, 2004, 199(1): 47-57.

[34] Banasik, A., et al.. Aluminum-induced micronuclei and apoptosis in human peripheral-blood lymphocytes treated during different phases of the cell cycle. Environmental Toxicology: An International Journal, 2005, 20(4): 402-406.

[35] McLachlan, D., et al.. Risk for neuropathologically confirmed Alzheimer's disease and residual aluminum in municipal drinking water employing weighted residential histories. Neurology, 1996, 46(2): 401-405.

[36] Zatta, P., et al.. Aluminium (III) as a promoter of cellular oxidation. Coordination Chemistry Reviews, 2002, 228(2): 271-284.

[37] Oberholster, P.J., et al.. Bioaccumulation of aluminium and iron in the food chain of Lake Loskop, South Africa. Ecotoxicology and Environmental Safety, 2012. 75: 134-141.

[38] Mussino, F., et al.. Primmorphs cryopreservation: a new method for long-time storage of sponge cells. Marine biotechnology, 2013, 15(3): 357-367.

[39] Cold Spring Harbor Laboratory Protocols. Calcium- and magnesium-free artificial seawater (CMF-ASW). Cold Spring Harbor Protocols 2009 December 1, 2009 [cited 2009 12]; pdb.rec12053]. Available from: http://cshprotocols.cshlp.org/content/2009/12/pdb.rec12053.short

[40] Duez, P., et al.. Statistics of the Comet assay: a key to discriminate between genotoxic effects. Mutagenesis, 2003.

[41] McKelvey-Martin, V., et al.. The single cell gel electrophoresis assay (comet assay): a European review. Mutation Research/Fundamental and Molecular Mechanisms of Mutagenesis, 1993, 288(1): 47-63.

[42] Koppen, G., et al.. The next three decades of the comet assay: a report of the 11th International Comet Assay Workshop. 2017, Oxford University Press UK.

[43] Elmore, A.R.. Final report on the safety assessment of aluminum silicate, calcium silicate, magnesium aluminum silicate, magnesium silicate, magnesium trisilicate, sodium magnesium silicate, zirconium silicate, attapulgite, bentonite, Fuller's earth, hectorite, kaolin, lithium magnesium silicate, lithium magnesium sodium silicate, montmorillonite, pyrophyllite, and zeolite. International journal of toxicology, 2003, 22: 37-102.

[44] Synzynys, B., A. Sharetskiĭ, O. Kharlamova. Immunotoxicity of aluminum chloride. Gigiena i sanitariia, 2004(4): 70-72.

[45] Varella, S.D., et al.. Mutagenic activity in waste from an aluminum products factory in Salmonella/microsome assay. Toxicology in vitro, 2004. 18(6): 895-900.

[46] Ingersoll, C.G., et al.. Aluminum and acid toxicity to two strains of brook trout (*Salvelinus fontinalis*). Canadian Journal of Fisheries and Aquatic Sciences, 1990. 47(8): 641-1648.

[47] Roberts, D.A., E.L. Johnston, A.G. Poore. Contamination of marine biogenic habitats and effects upon associated epifauna. Marine Pollution Bulletin, 2008, 56(6): 1057-1065.

[48] Rainbow, P., S. Luoma. Metal toxicity, uptake and bioaccumulation in aquatic invertebrates—modelling zinc in crustaceans. Aquatic toxicology, 2011. 105(3-4): 455-465.

[49] Rosseland, B., T.D. Eldhuset, M. Staurnes. Environmental effects of aluminium. Environmental Geochemistry and Health, 1990. 12(1-2): 17-27.

[50] Wood, C., et al.. Physiological evidence of acclimation to acid/aluminum stress in adult brook trout (*Salvelinus fontinalis*). 1. Blood composition and net sodium fluxes. Canadian Journal of Fisheries and Aquatic Sciences, 1988, 45(9): 1587-1596.

[51] Bergman, H. and J. Mattice, Lake acidification and fisheries project: acclimation to low pH and elevated aluminum by trouts. Canadian Journal of Fisheries and Aquatic Sciences, 1991. 48(10): 1987-1988.

[52] Wang, Z., J.P. Meador, K.M. Leung. Metal toxicity to freshwater organisms as a function of pH: A meta-analysis. Chemosphere, 2016, 144: 1544-1552.

[53] Iwegbue, C.M., et al.. Distribution, sources and ecological risks of metals in surficial sediments of the Forcados River and its Estuary, Niger Delta, Nigeria. Environmental Earth Sciences, 2018. 77(6): 227.

[54] Ipeaiyeda, A., N. Umo, and G. Okojevoh, Environmental Pollution Induced By an Aluminium Smelting Plant in Nigeria. Glo. J. Sci. Front. Res. Chem, 2012. 12(1).

[55] Kádár, E., et al., Avoidance responses to aluminium in the freshwater bivalve Anodonta cygnea. Aquatic Toxicology, 2001. 55(3-4): 137-148.

[56] Bondy, S.C. and A. Campbell, Aluminum and neurodegenerative diseases, in Advances in Neurotoxicology, Elsevier, 2017: 131-156.

[57] Hartwig, A.. Current aspects in metal genotoxicity. Biometals, 1995, 8(1): 3-11.

 DOI: https://doi.org/10.30564/jms.v2i1.1070

BILINGUAL PUBLISHING CO.
Pioneer of Global Academics Since 1984

Journal of Marine Science
http://ojs.bilpublishing.com/index.php/jms

ARTICLE

The Effect of ENSO on Hydrological Structure and Environment in the South Central Coast – Vietnam

Pham Xuan Duong[1*] Hoang Trung Du[1] Vo Tran Tuan Linh[1,2] To Duy Thai[1] Phan Minh Thu[1,3*]

1. Institute of Oceanography, Vietnam Academy of Science and Technology (VAST), Nha Trang, Vietnam
2. State Key Laboratory of Estuarine and Coastal Research (SKLEC), East China Normal University, Shanghai, China
3. Graduate University of Science and Technology, VAST, Ha Noi, Vietnam

ARTICLE INFO

Article history
Received: 14 September 2019
Accepted: 30 September 2019
Published Online: 29 December 2019

Keywords:
Effect of ENSO
Hydrodynamic regime
South Central Coast – Vietnam

ABSTRACT

ENSO (El Niño-Southern Oscillation) phenomena have impacted on the hydrodynamic regime and environmental factors of the tropical ocean in general. In case of Vietnamese South-Central Waters, impacts of ENSO only focused on issues of changing seasonal wind, seawater temperature anomalies, changing of water masses as the air-sea interaction. Based on several data sets collecting in the period of 2003-2017, new finding of seawater temperature, salinity and environmental factors was identified in the water masses of Vietnamese South-Central Waters. The highest salinity was 35.4 ‰. During the El Nino event, increasing water temperature and salinity caused to move the deeper water masses to be closer to the sea surface than that initial depth in the neutral period. During the La Nina event, the temperature of most water masses reduced by 0.1-3.0℃, and then these water masses could be affected to the deeper layer. During the phase from strong ENSO event towards the neutral time, nutrient salts of the 4 water masses were lower concentration in the neutral year, causing the lack of phosphorus in sea surface water masses.

1. Introduction

The El Niño–Southern Oscillation (ENSO) called a climate phenomenon that varies between Neutral, La Niña or El Niño phases, including changes of sea surface temperature over the tropical central and eastern Pacific Ocean [1-4]. The temperature changes significantly linked to major climate fluctuations around the world and caused the extremely weather. The pattern of El Niño has changed dramatically with the first El Niño events recorded over the last 400 years and El Niño events become more intense in last few decade [5]. Three strongest El Niño events were recorded as 1982-82, 1997-98 and 2015-16 (https://ggweather.com/enso/oni.htm), in which the 2015-16 El Niño events was the longest one . The 2015-16 El Niño events caused seri-

**Corresponding Author:*
Pham Xuan Duong,
Institute of Oceanography, Vietnam Academy of Science and Technology (VAST), Nha Trang, Vietnam;
Email: duongpx63@yahoo.com ;
Phan Minh Thu,
Institute of Oceanography, Vietnam Academy of Science and Technology (VAST), Nha Trang, Vietnam; Graduate University of Science and Technology, VAST, Ha Noi, Vietnam;
Email: phanminhthu@vnio.org.vn

DOI: https://doi.org/10.30564/jms.v2i1.1215

ous disasters on the global [6]. During this event, coastal provinces in the South-Central Vietnam had to declare natural disasters due to insufficient rainfall, high temperature causing drought –stricken areas. Especially, in November, 2017, typhoon Damrey with winds of up to 12 levels (Bopho Scale) destroyed both land–based source and ocean.

The ENSO events were influenced to the hydrological structure and marine environment in the South-Central Waters of Vietnam. Results focused the features of wind during the monsoon season, as well as the abnormal periods of climate. Chung and Long [7] reported the temperature anomalies and the mechanism of water level changed by the effect of ENSO, the abnormal increases of temperature and the abnormal decreases of wind speed, which cause the weakness of upwelling in the South-Central Region. Dipper [8] revealed that water bodies was influenced by seasonal variations. Xuan [9] reported that based on the collection of large data on temperature and salinity and T-S curve analysis determined the relations between the surface water mass and seasonal air temperature in the Southeast sea of Vietnam. Anomalous surface water temperature and salinity during the period of ENSO were as -4°C and +1.2 ‰, respectively [10,11]. Water mass with temperature anomalies affected the aquatic trophic structure [12,13]. During the uptake phase, the nutrient-enriched layers were concentrated in a clearly and relatively broad mass, with high nutrient content of the watershed [13]. ENSO also affected nutrient structures through effects on the phytoplankton community [14], food webs [15] and the elements of wind, rain, storms, temperature [16,17]. Upwelling phenomena declined sharply in the El Nino years [8]. The on/offshore of Ninh Thuan - Binh Thuan are quite affected by ENSO phenomena [13].

The paper found new score of hydrological structure and the environment during the phases of the ENSO phenomenon in the marine of South Central region of Vietnam.

2. Methodology

2.1 Data Set

Data sources were collected from Vietnam-USA joined project (2013-2016) (Figure 1), International Project Cooperation under the Vietnam-Germany protocols from 2003-2007 (Figure 2) and project "Changes of wind characteristics, air temperature and hydrological structure in Ninh Thuan - Binh Thuan Waters in ENSO years" (2016-2017) (Figure 3).

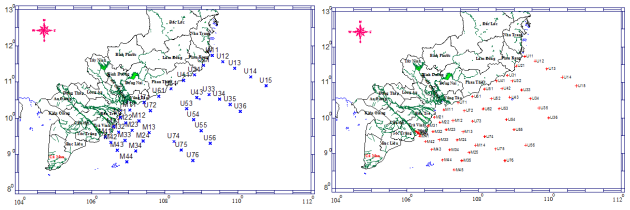

Figure 1. Sampling stations under Vietnam-USA joined project (left: in Northeast monsoon; right: Southwest Monsoon)

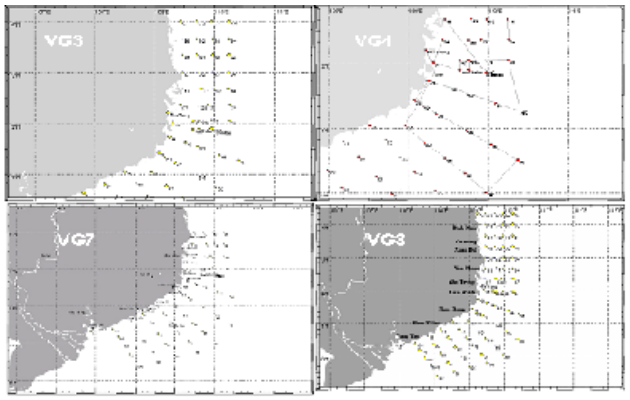

Figure 2. Sampling stations under Vietnam-Germany Cooperation projects: (a): VG3; (b): VG4; (c): VG7; and (d): VG8

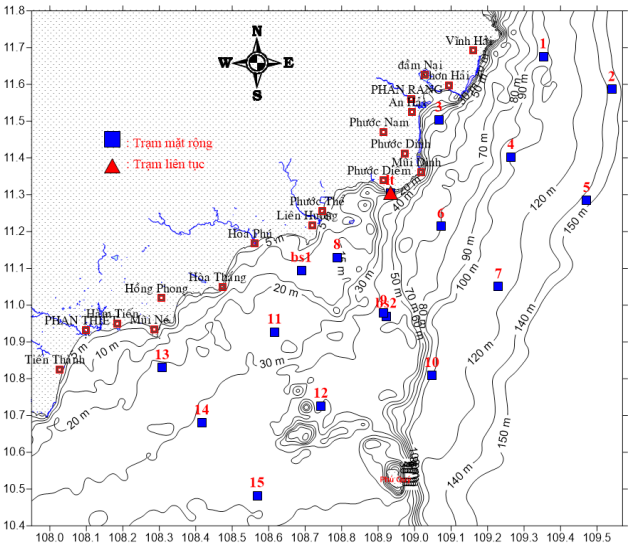

Figure 3. The map of sampling station in 2016 and 2017

In addition, data from the HYCOM + NCODA Global Reanalysis database, with high resolution 0.08° from 2002 - 2012 (11-year period) and from Aug. 2016 – Aug. 2017 were used for corrected with two surveys during ENSO years. The aggregate data on the vertical distribution of temperature - salinity structure (Wang *et al.*, 2016) with average values of several months from 1919 to 2014 in the South China Sea was combined in this analysis. Monthly

 DOI: https://doi.org/10.30564/jms.v2i1.1215

average Nino index was collected from https://ggweather.com/enso/oni.htm.

2.2 Data Analysis

Temperature and Salinity profile and T-S diagram were analyzed with Mamayev [18] by using Matlab R2013a software. Using the statistical method to study the average fluctuation in the South Central Marine of Vietnam through the extreme analysis of standard deviation and specific time of extreme occurrence, average of the whole process.

3. Results and Discussion

3.1 The Influence of ENSO Phenomenon on Hydrological Structure in Water Masses in South Central Marine of Vietnam (SCMV)

Base on the TS-diagram and physical characteristics of the water layers, we identified the 10 water masses in SCMV from different origins (Table 1 and Figure 4). DW water had salinity of 34.4 psu and temperature of less than 04 ^{o}C and relatively stable with a water density of about 1027.6 kg/m^3. PTW water which exist in the depth of 400-700m had a temperature range of about 7-10°C, salinity of 34.2-35.0 psu. Between two these water masses, WM1 water had the characteristics of both DW and PTW water with temperatures in the range 4-7°C, salinity of 34.3-35.8 psu. MSW water found in the SCCV had a salinity of not less than 34.1 psu. This water layer was relatively close to the surface of the sea with a temperature of 16.5-20°C. This water mass interacts with PTW water in the deeper water to create a WM2 disturbance in the depth range of 100-450m with a temperature of 10-16.5°C and salinity ranging from 34.1-35 psu. The OSW water has a functional activity from the surface down to 90m with a salinity of 33.7-34.8 psu and a temperature of 25-30.5 °C. This OSW water also interacts with maximum salinity water to create WM3 water, which is mixed between MSW and OSW water. This mixing water was found from the surface layer down to a 180 meters and the temperature range was about 19-28°C and the salinity was in the range of 33.9-34.8 psu. As the water masses depend mainly on the current regime, so in the southwest monsoon season it cannot exclude the effects of water from the Mekong River and the Gulf of Thailand (MKGTW) in the study area, especially from south Binh Thuan to Vung Tau province. This water mass had a range of activity from the surface down to 60m in depth and has a salinity of no more than 32.9 psu. The temperature of this water was quite high from 27-31.5°C. EJW mainly occurs during the southwest monsoon season from the Karimata strait, which has a high temperature of 25.5-31°C and a salinity of 32.5-33.7 psu. The last ECSW water origined from the East China Sea appears to be predominantly in the northeast monsoon with relatively low temperatures of 21-25° C, salinity of 33.2-33.9 psu.

Table 1. Characteristics of water mass in South Central Marine of Vietnam [19]

No.	Watermasses	Temperature (^{o}C)	Salinity (psu)	Layer depth (m)
1	Deep Water (DW)	<4	>34.4	>1,200
2	Permanent Thermocline Water (PTW)	7-10	34.2-35.0	400-700
3	Mixing of DW and PTW (WM1)	4-7	34.3-35.8	700-1200
4	Maximum Salinity Water (MSW)	16.5-20	>34.1	50-250
5	Mixing of PTW and MSW (WM2)	10-16.5	34.1-35.0	100-450
6	Offshore Water (OSW)	25-30.5	33.7-34.5	0-90
7	Mixing of MSW and OSW (WM3)	19-28	33.9-34.8	0-180
8	Mekong River and Gulf of Thailand Water (MKGTW)	27-31.5	<32.9	0-60
9	Equator and Java Sea Water (EJW)	25.5-31	32.5-33.7	0-80
10	East China Sea Water (ECSW)	21-25	33.2-33.9	0-80

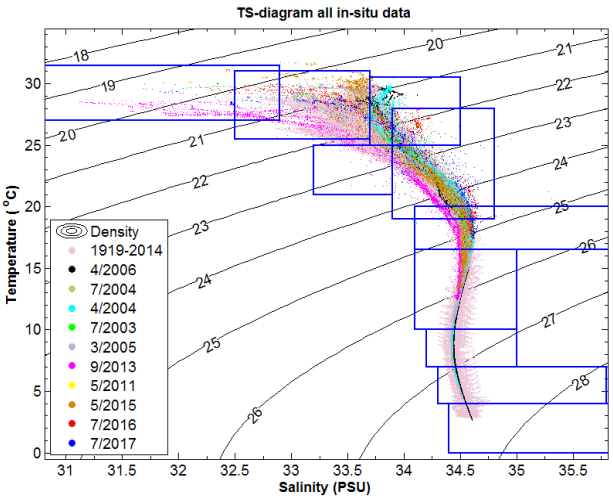

Figure 4. TS-diagram and typical distribution of water masses [19]

The influence of ENSO phenomenon on hydrological structure can be seen in all temperature profiles (Figure 5). The temperature was reached the highest value in May 2015 (brown line) at about 30-31.5 °C. In Vietnam records after two period of heat due to the influence of El Nino showed that average temperature in May 2015 is higher than average of several years about 2-3°C. Moreover, the salinity profile in 2016 at the Station 1 (located at longitude 109.3540^{o}E, latitude 11.6707^{o}N, Figure 5) revealed that salinity reached the value up to 35.4 psu. That salinity is the highest in the historical data series.

DOI: https://doi.org/10.30564/jms.v2i1.1215

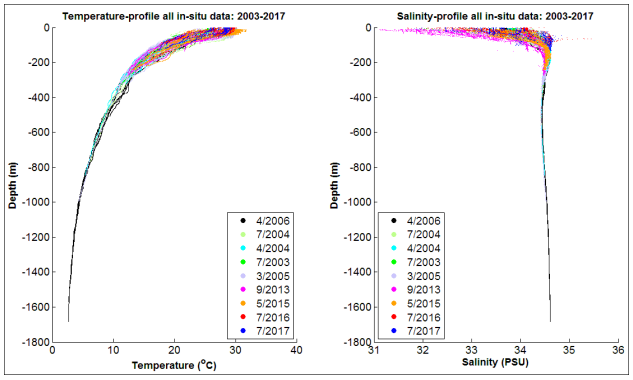

Figure 5. Vertical distribution of temperature and salinity from in-situ data in the South Central Marine of Vietnam [19]

Through the indicators of water body characteristics, the results of the variation of water masses over time and the depth distribution showed that in 2004 the presence of all water bodies was found in the South Central region, and in 2006 the presence of DW had a temperature in the range 2.7-4.0°C, and high salt content in the range 34.5-34.6 psu. In 2015 MKGTW had not much impact to the South-Central region because of the hot and dry weather last year in the South China Sea. In 2016 – 2017. Results of the six water bodies in the South-Central Coast indicated that surface water masses of OSW, EJW, ECSW and MKGTW had lower temperatures than that of basins in 2015 by around 0.5° C, but some salinity values are high up to 35.4 psu.

Influence of El Nino: The most obvious impact on surface water mass, such as the MKGTW, increases the water temperature by 0.4-0.7 ° C. Besides, offshore water mass, which is from the Western Pacific, are also affected by El Nino warmer 0.6°C while salinity also increases by 0.2psu. Under the impact of El Nino, salinity increased and water masses were pushed upward the surface about 80m to versus position depth in neutral phases. However, the blocks of deep water, PTW and DW were less influenced by El Nino. On the other hand, the impact of El Nino depends on their strength which is reflected in the variation of the water mass. Obtained data in July 2003 (moderate El Nino) and July (very strong El Nino) showed large fluctuations of the water depth (Table 3.2). Almost all of the waters distributed in the deeper layers tend to be pushed closer to the surface than in the strong El Nino period (2016) from a few meters up to tens of meters.

The influence of La Nina: The indicator of the effect of La Nina is water temperature. Almost all of the water masses in a strong La Nina period decreased temperature quickly from 0.1°C (WM2 water) to 3.0°C (WM3 water). Surface water masses as the MKGTW water decreased temperature by 1.4°C. However, there are some anomalies in that La Nina increased the temperature in water mass of ECSW, OSW, WM2 to 0.1 - 0.2°C. This confused result needs further study. Similar to El Nino's impact, La Nina also pushed PTW and WM1 to deeper water but raised MSW and WM3 to the surface of the sea by 40-50m. The remaining water masses have a small variation in the depth stratification with only a few meters in the sea.

Table 2. The influence of ENSO on hydrological structure in each water mass [19]

No.	Water mass	El Niño			La Niña		
		Temperature (°C)	Salinity (psu)	Layer depth (m)	Temperature (°C)	Salinity (psu)	Layer depth (m)
1	DW	#	#	#	#	#	#
2	WM1	-1.0	0	+(30-50)	-1.4	+0.1	+(30-50)
3	PTW	0	0	+(30-50)	0	0	+(30-50)
4	WM2	+0.4	0	-75	-0.1	+0.1	#
5	MSW	+1.2	+(0.2-0.6)	-80	+1.0	-(0.1-0.2)	-(40-50)
6	WM3	0	+0.2	-70	-3.0	-0.2	-(30-50)
7	OSW	+0.6	+0.2	-30	-2.0	+0.2	-3
8	EJW	-0.4	0	-14	-0.5	0	-6
9	ECSW	-(0.4-0.6)	-0.1	-30	-2.5	+0.1	+20
10	MK-GTW	+(0.4-0.7)	-0.3	-15	-0.4	-0.2	-2

Note: + increasing - decreasing (+ depth) means deeper; (- depth) means shallower

3.2 Influences of ENSO on the Nutrient Structure in Water Masses

The Ocean Nino Index (ONI) indicator shows that during the period 1998 - 2016, the nutrients in the water bodies were not variable (Figure 6). All of the highest and lowest values of the DIN / DIP ratios (96.4 in 2000 and 6.5 in 2011), Si / DIN (7.7 in 2011 and 0.4 in 2000), Si / DIP (253.1 in 1998 and 11.2 in 2011) were recorded at the time of the La Nina phenomenon (02/2000 and 11/1998, ONI = -1.4 and - 1,3).

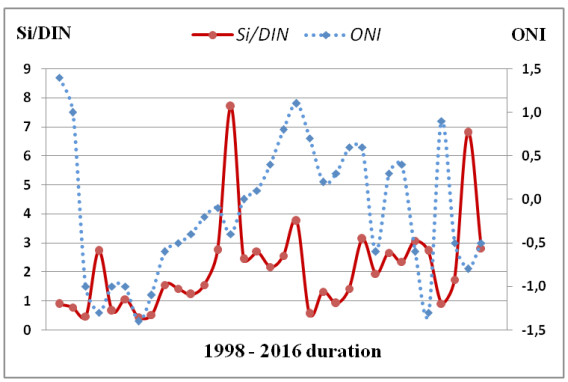

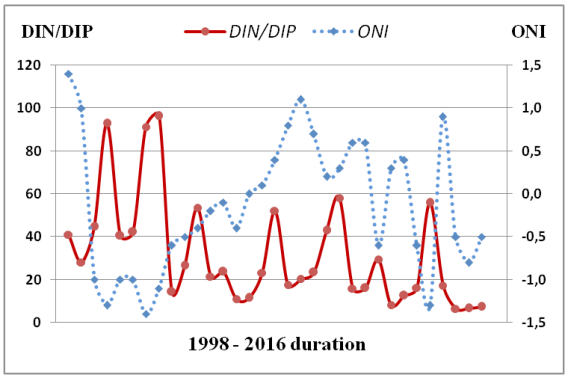

Figure 6. Si/DIN (left) and DIN/DIP (right) ratios to ONI over time

The results also showed that at the South Central the decline or accumulation of Si in sediments was not observed to change predominant species from diatoms to green algae or cyanobacteria (Figures 7, 8).

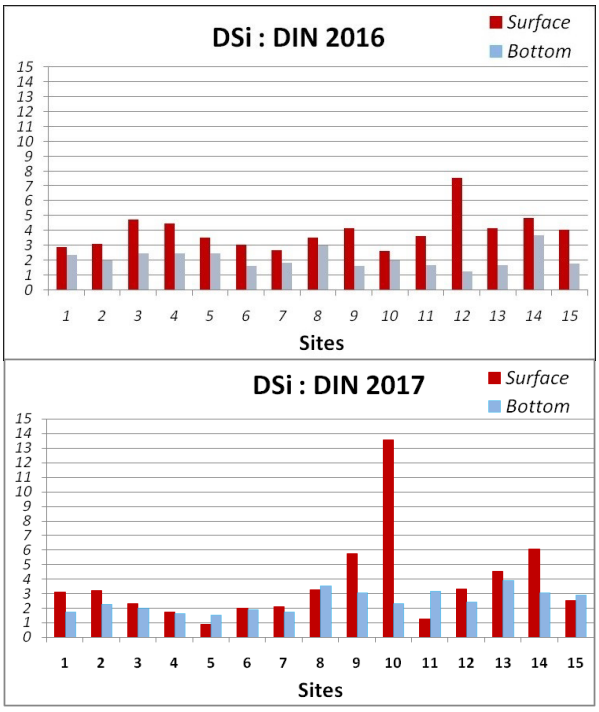

Figure 7. Chart of DSi/DIN ratio with stations in Figure 3

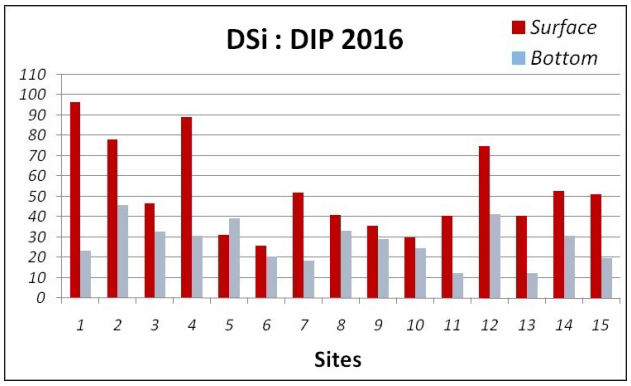

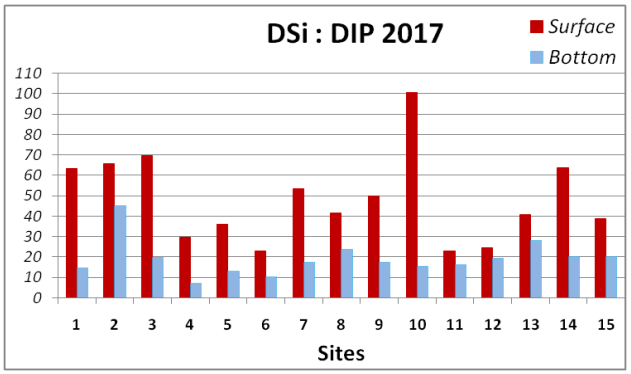

Figure 8. Chart of DSi/DIP ratio with stations in Figure 3

In the strong El Nino year (2016), there was a shortage of P in the surface with very low DIP concentrations and the DIP and DSi/DIP ratios were always more than 22. However, the mean values of molar ratios showed that there was a shortage of N at the bottom (Figure 9). In neutral year (2017), there was a shortage of P, N in some surface layers.

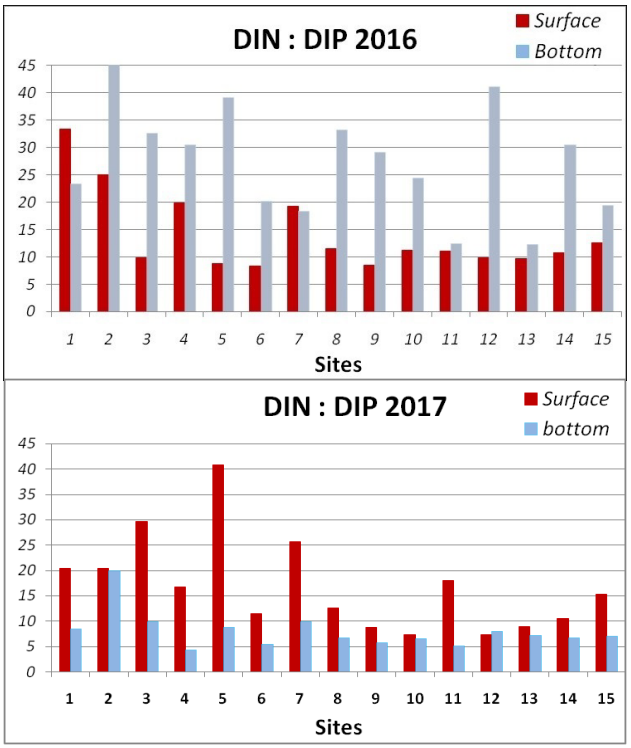

Figure 9. Chart of DIN/DIP ratio with stations in Figure 3

Nutrient characteristics in water masses: In general, the concentration of nutrient salts in most of the water bodies recorded in the neutral year is higher than in the active year of El Nino. Chart of distributed by depth showed that in El Nino years the water mass was pushed upward, but nutrient concentrations were lower than in neutral year (Figure 10-12). In MKGTW, the El Nino year was higher (9.78 µM) and the DSi / DIN, DSi /DIP ratios were both

DOI: https://doi.org/10.30564/jms.v2i1.1215

higher than those in the neutral year; but the DIN / DIP ratio was lower (12.46). In the remaining water bodies, although the levels of nutrient salts in El Nino year are lower than the neutral year, the molar ratios are not in the similar variation.

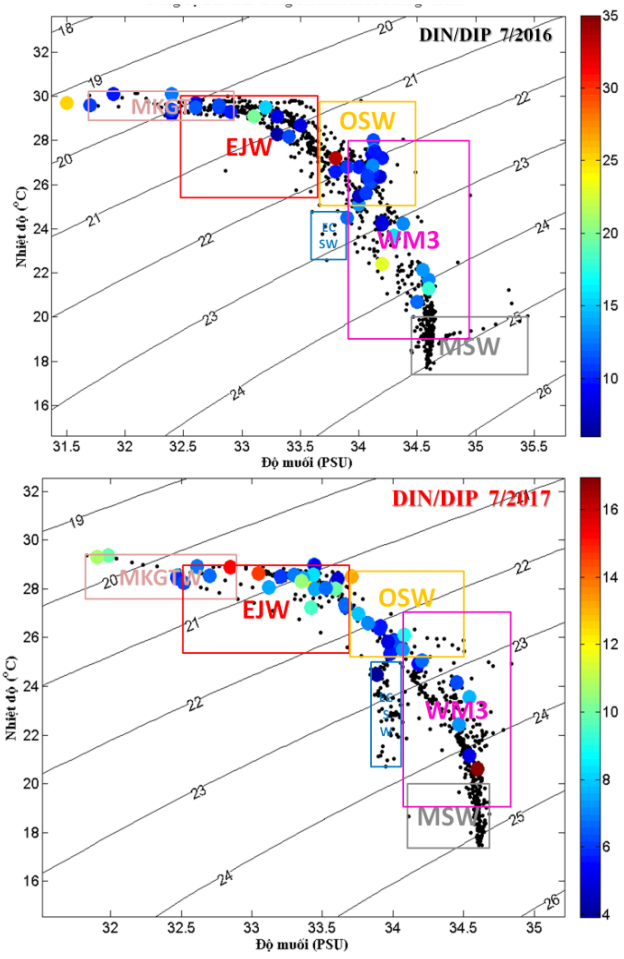

Figure 10. DIN/DIP ratio of water the masses recorded through the two surveys

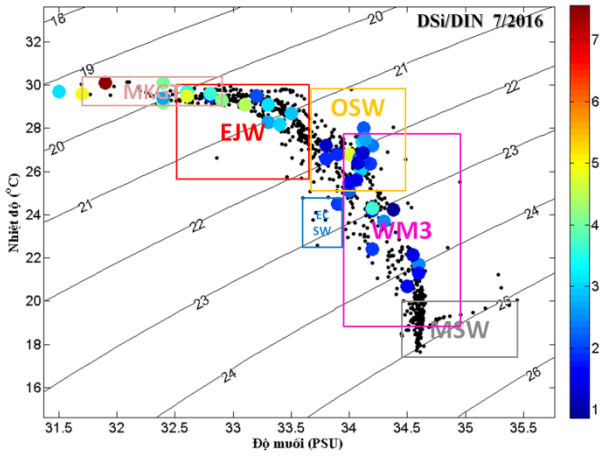

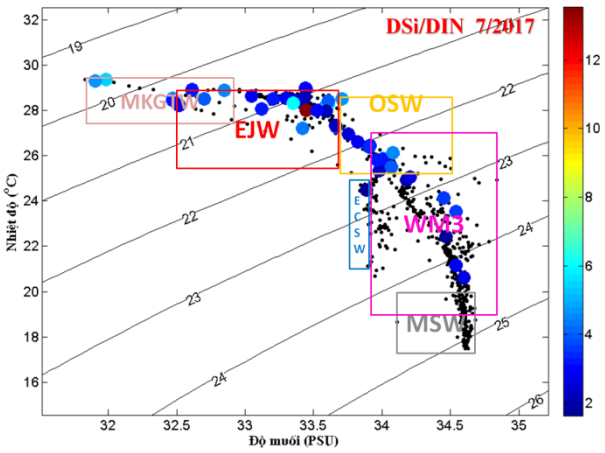

Figure 11. DSi/DIN ratio of water the masses recorded through the two surveys

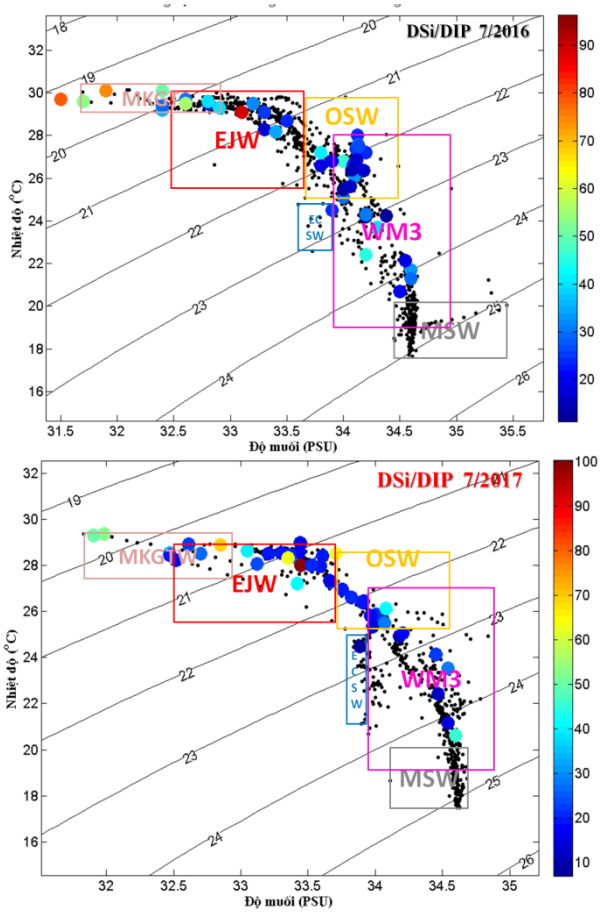

Figure 12. DSi/DIP ratio of water the masses recorded through the two surveys

4. Conclusion

Based on the results of analysis collected in the period of 2003-2017, the paper found (1) Highest salinity 35.4 psu in 10 water masses in the south central marine in strong

 DOI: https://doi.org/10.30564/jms.v2i1.1215

El Nino year; (2) El Nino increased the salinity and temperature of water masses and pushed the upper masses closer to the surface from a few meters to 10 of meters; (3) La Nina decreased temperature and salinity from 0.1^0C to 3.0^0C and increased water exchange by ECSW anomalies, OSW, WM2 and increased temperature of 0.1 - 0.2^oC over the period of La Nina; (4) All of the highest value and lowest ratio of the DIN / DIP, Si / DIN, Si / DIP were recorded aduring the La Nina period; and (5) The nutrient concentrations in the water masses in neutral years were higher than those in strong El Niño year.

Acknowledgements

This work is funded by projects of ĐTĐL.CN.17/28, Institute of Oceanography projects in 2016-2017 and VT-UD.12/18-20. We would like to thank Prof. Bui Hong Long, the coordinator of the Vietnam-USA joined project (2013-2015) and the Vietnam-Germany joined projects (2003-2007) for sharing the in-situ data of physical-hydrological and environmental features.

References

[1] Barr, C., Tibby, J., Leng, M.J., Tyler, J.J., Henderson, A.C.G., Overpeck, J.T., Simpson, G.L., Cole, J.E., Phipps, S.J., Marshall, J.C., McGregor, G.B., Hua, Q. & McRobie, F.H.. Holocene El Niño–Southern Oscillation variability reflected in subtropical Australian precipitation. Scientific Reports, 2019, 9: 1627.

[2] Dai, A. & Wigley, T.M.L.. Global patterns of ENSO-induced precipitation. Geophysical Research Letters, 2000, 27: 1283-1286.

[3] McPhaden, M.J., Zebiak, S.E. & Glantz, M.H.. ENSO as an Integrating Concept in Earth Science. Science, 2006, 314: 1740-1745.

[4] Soulard, N., Lin, H. & Yu, B.. The changing relationship between ENSO and its extratropical response patterns. Scientific Reports, 2019, 9: 6507.

[5] Freund, M.B., Henley, B.J., Karoly, D.J., McGregor, H.V., Abram, N.J. & Dommenget, D.. Higher frequency of Central Pacific El Niño events in recent decades relative to past centuries. Nature Geoscience , 2019, 12: 450-455.

[6] Zhai, P., Yu, R., Guo, Y., Li, Q., Ren, X., Wang, Y., Xu, W., Liu, Y. & Ding, Y.. The strong El Niño of 2015/16 and its dominant impacts on global and China's climate. Journal of Meteorological Research, 2016, 30: 283-297.

[7] Chung, T.V. & Long, B.H.. Influence of temperature field and abnormal changes of water level in the South China Sea related to climate change. Journal of Marine Science and Technology, 2016, 16: 44-52.

[8] Dippner, J.W. & Loick-Wilde, N.. A redefinition of water masses in the Vietnamese upwelling area. Journal of Marine Systems, 2011, 84: 42-47.

[9] Xuan, N.B.. Study on the formation and distribution of surface water bodies in the East Sea. Proceedings of the International Conference "Bien Dong 2012". Nha Trang, Vietnam, 2013: 183-190.

[10] Bai, L.V. & Lanh, V.V.. Characteristics of distribution and structure of saline water in strongly rising waters. Proceedings of the study on the highly developed South Central waters, 1997: 39-48.

[11] Lanh, V.V.. Thermohaline structure and water masses of South China Sea. Collection of Marine Research Works VI, 1995: 25-35.

[12] Lalli, C.M. & Parsons, T.R.. Biological Oceanography: An Introduction. Oxford: Elsevier Publications, 1997.

[13] Long, B.H.. The phenomenon of rising water in Vietnamese waters. Natural Science and Technology Publishing House, 2009.

[14] Doan-Nhu, H., Nguyen-Ngoc, L. & Nguyen, C.-T.. ENSO and anthropogenic impacts on phytoplankton diversity in tropical coastal waters. Progress in Oceanography, 2016, 140: 1-13.

[15] Zhao, H., Zhao, J., Sun, X., Chen, F. & Han, G.. A strong summer phytoplankton bloom southeast of Vietnam in 2007, a transitional year from El Niño to La Niña. PLOS ONE 13, e0189926, 2018.

[16] Vu, T.V., Nguyen, H.T., Nguyen, T.V., Nguyen, H.V., Pham, H.T.T. & Nguyen, L.T.. Effects of ENSO on Autumn Rainfall in Central Vietnam. Advances in Meteorology, 2015, 12.

[17] Thao, P.T.P., Minh-Thu, P., Giam, N.M., Duan, H.D. & Long, B.H.. Relationship between Drought and Rainfall Due to Tropical Cyclone and Depression in Ninh Thuan, Vietnam. Current Journal of Applied Science and Technology, 2018, 30: 1-8.

[18] Mamayev, O.I.. Temperature - Salinity Analysis of World Ocean Waters. Elsevier B.V., 1975: 374.

[19] Thai, T.D., Long, B.H., Tuan, N.V., Cong, N.C., Bac, P.T., Hoi, N.T.T., Thinh, N.D. & Dung, N.T.T.. Some study results on the characteristics and variability of water masses in the south central Vietnam. Journal of Marine Science and Technology, 2018, 18: 1-12.

DOI: https://doi.org/10.30564/jms.v2i1.1215

BILINGUAL PUBLISHING CO.
Pioneer of Global Academics Since 1984

Journal of Marine Science
http://ojs.bilpublishing.com/index.php/jms

REVIEW

Can Air Quality be Influenced in Coastal Areas by Shipping?

Vasile Rata Eugen Rusu*

Department of Mechanical Engineering, "Dunarea de Jos" University of Galati, 47 Domneasca St., 800 008 Galati, Romania

ARTICLE INFO

Article history
Received: 8 October 2019
Accepted: 23 October 2019
Published Online: 29 December 2019

Keywords:
Air quality
Black Sea
Particle matter
Shipping emissions
Sustainability

ABSTRACT

The problem of pollution is a topical issue at global, regional but also at the local level. Starting from this idea, the question arises whether the coastal region in the North-East of the Black Sea is affected by the emissions resulting from the combustion of marine fuels in large ship engines, which manage to set in motion floating buildings intended for the transport of goods and passengers. This paper wants to evaluate the variation of the air quality indicators in the coastal area of Romania, taking into account the contribution that the ships by their number, size and destination can have on these qualitative factors. Such an approach is needed from the perspective of the more than 500,000 inhabitants possibly affected by the effects with which this industry is accompanied. As the Black Sea active fleet is already old, as its ages year by year, the premises for the need for this study can be set up. As in other regions, drastic measures are taken in order to reduce the effects of pollution due to such economic activity, the assessment of the effects that this industry produces in inhabited areas becomes necessary. In order to carry out this study, air quality data from the database provided by the National Air Quality Monitoring Network of the Workshop on the calitateaer.ro site were evaluated.

1. Introduction

At the European level, the issue of pollution is one of the priorities addressed and assumed by the European decision-making institutions.. In this regard, a series of measures are taken to mitigate the side effects that result from this harmful action to the environment. These measures are most often taken in force, based on strict monitoring periods, scientific, technical and economic evaluations aimed at determining the best solutions for limiting the side effects of pollution.

The effects of pollution act on the medium and short term by reducing the quality of life of living beings in the affected areas and in the long term through climate change. It is known that pollution in its various forms has direct effects on human health. The air quality is strictly influenced by air pollution, by changing the characteristics of the physio-chemical composition of the air. The most common process that influences air quality parameters is the combustion phenomenon. The combustion of fossil fuels is carried out for both industrial and domestic use. For industrial purposes, the combustion of fuels is used for the purpose of producing electricity, heating agent, freight transport by different means: road, rail, sea, air, passenger transport, etc.

According to the data provided by the International Maritime Organization (IMO) shipping (Shipping Indus-

**Corresponding Author:*
Eugen Rusu,
Department of Mechanical Engineering, "Dunarea de Jos" University of Galati, 47 Domneasca St., 800 008 Galati, Romania;
Email: erusu@ugal.ro

 DOI: https://doi.org/10.30564/jms.v2i1.1287

try) is a major producer of greenhouse gas emissions, with this economic sector being assigned 2.5% of the global greenhouse gas emissions.

In this context, the European Community has already implemented a number of European directives, with applicability, reducing greenhouse gas emissions by 20% by 2020 compared to the volume of emissions from the early 1990s [1]. In the field of maritime transport, the European Maritime Safety Agency (EMSA) represents the European entity with a role in the implementation of the above-mentioned decisions, the same agency aims to implement the monitoring, control and verification (MRV) process at the member country level [2].

However, the volume of emissions resulting from the transport of goods by sea will increase in the coming years, it is supposed till 2050 exist a potential of increasing from 50 to 250% depending of various scenarios, due to the trend of world trade. This will lead to an increase in the total volume of emissions from shipping, in the last IMO report is mentioned that the shipping is responsible for 2.5% annually from globally greenhouse gas emissions [3].

2. North-West Coast Area of the Black Sea

It is known that in general the shipping routes [4] are described, where it is possible, by the representation of the shores limit. In particular, even if the vessels did not have defined as navigation specification the coastal area, they often follow a direction parallel to the shore, but as close to the shore as possible. The Black Sea is characterized by the movement of goods by sea over short distances, according to Eurostat over 70% of voyages have this feature. According to the same Eurostat studies, we understand that the trend in the field of freight transport by water is increasing in the studied area. Constanta Port occupying the 18th position in a European top as importance, being taken into account the volume of cargo that transited this port. At the same time, the port of Constanța occupies the 5th position in the same top for the volume of bulk cargo that used the port services [5]. The trend of increasing the volume of goods, but also of the number of ships transiting the Black Sea region is also supported by the global direction which shows that in the period 1950-2001 the world fleet of active ships tripled its number [6].

Figure 1 shows the concentration of the navigable routes in the North-West area of the Black Sea. The bright red color represents critical points, where the route is intensely used. This map is created based on GPS location data, delivered by satellite for 2017 and processed by marinetraffic.com [7].

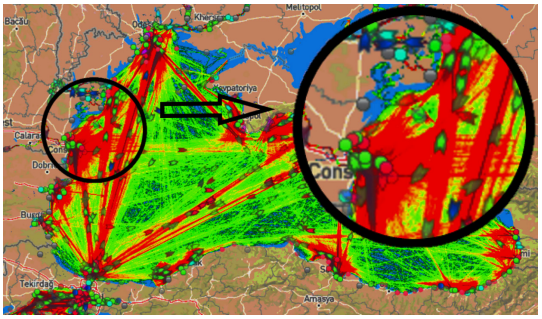

Figure 1. North-West shipping routes in the Black Sea [8]

Every day, the region is transited by over 300 ships, due to a considerable number of ports on the Romanian shoreline, from which can be mention: Constanta Port, Mangalia, Agigea, Midia-Năvodari, Sulina. Ships that voyage destination the Ukrainian region of Odessa and come from Bulgaria or the Bosphorus Strait, also transit the round perimeter shown in Figure 1. This number represents approximately 40% of the total volume of naval traffic carried out throughout the Black Sea area.

The Black Sea active fleet can be characterized as aging, poorly technized criteria resulting from a series of randomly selected batches of vessels [7]. An important number of these ships (36%) were built before 1990, when the rule was imposed that the composition of Sulfur in fuel should not exceed 4.5%. 55% of the ships were built before 2000, when the TIER I regulation on NOx emissions was imposed. Over 85% of the identified vessels were built before 2010, the year in which the TIER II regulations regarding NOx emissions and the rule that refers to the percentage of Sulfur in fuel that should not exceed more than 3.5% were imposed.

The North-West of the Black Sea is represented by the coast of Romania, shown in Figure 2, where we find a series of urban settlements and numerous rural settlements. The area considered the purpose of the study being delimited by the 245km long Romanian shoreline, with a depth of 30km inside the terrestrial area. According to the latest maps, the marked area is totaling around 5500 square km, except for the lake areas.

DOI: https://doi.org/10.30564/jms.v2i1.1287

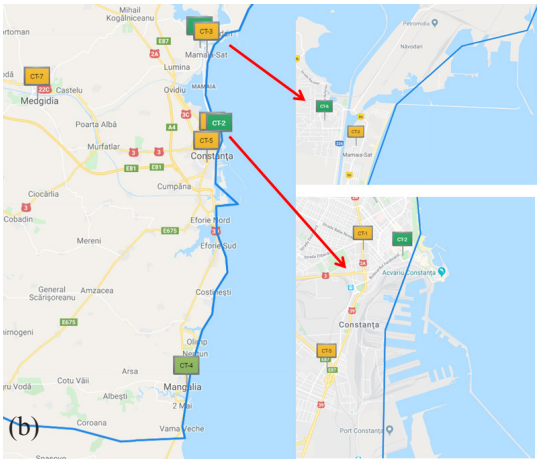

Figure 2. (a) The Romanian coastal area affected by shipping emission from Black Sea [9], (b) the position of the monitoring station located in Constanta County [10]

According to the data in table 1, on the Black Sea shore in Romania there are over 412,000 people living in the urban area, about half a million summing up the rural area.

Table 1. The number of inhabitants possibly affected by shipping emissions in Black Sea, Romanian shore

County	City	No. of inhabitants
Constanța	Constanța	306332
	Mangalia	40740
	Năvodari	34337
	Ovidiu	13490
	Eforie	9555
	Techirghiol	7034
Tulcea	Sulina	3663

3. Air Pollutant Compounds

National Air Quality Monitoring Network webpage [10] provides information about the air quality, showing in real-time the specific indicators (specific index) of air quality for the following pollutants: sulfur dioxide (SO2), nitrogen dioxide (NO2), particulate (PM10) and carbon monoxide (CO). Some limits are there indicated for each pollutant, starting with which the bad quality of the air is considered. These limits are: for SO2 is 350 μg/m^3, for NO2 is 200 μg/m^3, for PM10 is 50 μg/m^3, while for CO is 10 mg/m^3.

On the territory of Constanta County there are 7 locations where the air quality is evaluated from the perspective of various parameters. All 7 locations are located in the perimeter bounded by the grid in Figure 2(a). Only 6 locations are near to the coastline and also in the proximity of the Romanian ports. These 6 locations are shown in Table 2. In Tulcea County there are not stations located near to the coast.

Table 2. Monitoring fix station situated on the Romanian coastal area (see also Figure 2b)

No.	ID sample station	Location
1	CT1	Constanța
2	CT2	Constanța
3	CT3	Năvodari
4	CT4	Mangalia
5	CT5	Constanța
6	CT6	Năvodari

3.1 COx Emissions

Carbon monoxides result from the burning of fossil fuels like: oil products and LNG. CO emissions are directly proportional to fuel consumption. Consumption can be reduced by modifying ship shapes that involve the reducing ship's resistance, the ship's resistance can be also improved by optimizing the appendix, using active solution like bubble air lubricant systems, propulsion system efficiency, and operational factors such as sea state knowledge which involve the route planning, speed regime of ship/fleet, etc.

From the perspective of CO emissions levels are not alarming, but it is worrying that there is a trend to increase the values and the recurrence number of the maximums recorded by the stations mentioned in Table 2. This statement is based on the evolution of the values recorded in the last 3 years [10].

3.2 NOx Emissions

Nitrogen oxides are a result of the reaction between two common chemical compounds, oxygen and nitrogen, in a medium with high temperature. The most common way of producing is by combustion of fuels, like the burning of fuel inside the engines. Massive marine engines represent a significant source of emissions. The amount of NOx resulting from combustion varies depending on the type of fuel (diesel, gas, etc.), the mechanical and operating conditions of the engine. There are systems for cleaning the resulting exhaust gases, used in practice even in the naval field and are called SCRs based on Catalyst-based. Tehse emissions can cause acid rains that are T contributing to the acidity of seas and oceans, because this gas is easily soluble in water.

3.3 SOx Emissions

Sulfur oxides are formed during the burning process in ma-

DOI: https://doi.org/10.30564/jms.v2i1.1287

rine engines, but not only, it appears because of presence of sulphur in the fuel. It is recognised as an emission that contributes to pollution and which is harmful to humans.

3.4 Particle Matter Emissions

PM emissions are associated with gas emission processes due to burning of fossil fuels and lubricating oils. These residual products of combustion are an international issue that threatens human health. These emissions are sometimes visible due to smoke and soot dimensions. On the other hand, the most dangerous of this kind of emissions are those that can be seen only with microscopic devices. These emissions cannot be detected without special measurement devices or detectors.

After the analysis of the data available data in each location presented in Table 2, for the last six years (from October 2014 until October 2019), only two locations (CT4 and CT5) were chosen for a graphical representation (Figure 3) because more data are available for all pollutants. Also, these stations are located near to the maritime ports where the ship's traffic is more intense. The station CT4 is located near to the Mangalia port, while the station CT5 is situated close to the Constanta port, the most important Romanian port. It can be also mentioned that in the other stations no worrying values were observed.

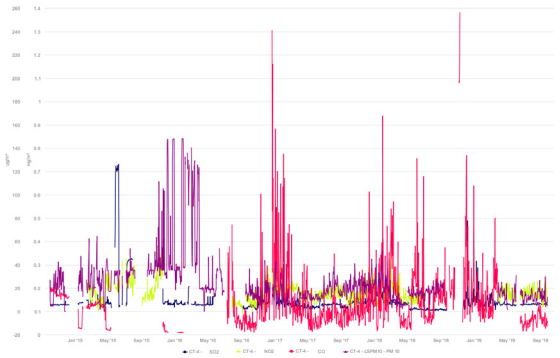

(a)

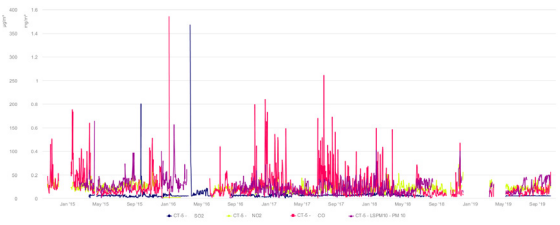

(b)

Figure 3. The pollutant emissions in Romanian coastal area measured at the stations CT4 (a) and CT5 (b), time period 1st October 2014 – 20th October 2019

From Figure 3 it can be observed that only PM10 emission values reached many times the worst index. It can be noticed that in 2016 at CT4 location for several times the PM10 emission was about three times higher than the limit value. In the case of CT5 location, there are some peaks in 2015 and 2016, but also there are various periods when the PM10 emission reaches the limit.

On October 4, 2019, a critical limit can be observed in Figure 4, namely the air quality index 5 which is related to the quantity of 50 µg / µg/m^3.

Name	Hourly index	Today index	Yesterday index
CO	1 0.08mg/m³ 2019/10/04 08:00:00	1 0.13mg/m³	1 0.14mg/m³
PM 10	5 52.50µg/m³ 2019/10/04 08:00:00	5 53.13µg/m³	4 47.08µg/m³
SO2	1 5.27µg/m³ 2019/10/04 08:00:00	1 5.47µg/m³	1 5.92µg/m³
O3	1 15.65µg/m³ 2019/10/04 08:00:00	2 47.92µg/m³	2 79.95µg/m³
NO2	1 18.78µg/m³ 2019/10/04 08:00:00	1 18.78µg/m³	1 28.28µg/m³

Figure 4. PM10 level alarm CT-5 site, time frame 04.10.2019

Following the wind rose (Figure 5) we can see that the predominant direction of the wind is from S and SSE, which indicates that the wind is blowing from the Constanta port and from sea. Taking into consideration that onshore there are no factories or other pollution sources than the usual car traffic, it reasonable to suppose that air pollution is coming from the sea, due to the maritime traffic and harbor operations.

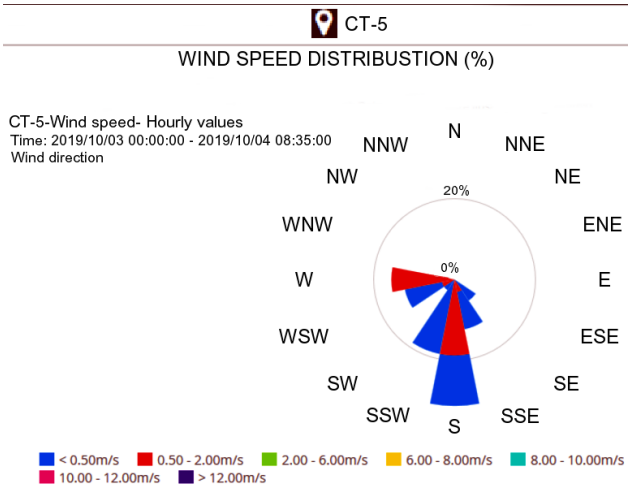

Figure 5. Wind speed and direction in CT-5 site

Numerous studies conducted for the Black Sea region show that a significant volume of pollutants is emitted into the air and has the origin of industries operating various types of ships [11-13]. They are of various categories as commercial ships, navy ships, special ships, etc.

According to a recent study [11] that evaluated total SOx and NOx emissions from shipping activities in the Black Sea region over a year, considerable values have resulted: 409.39

DOI: https://doi.org/10.30564/jms.v2i1.1287

kilo tonnes NOx compared to an active fleet of 720 vessels operating 8000 hours a year in the Black Sea region. The same operating conditions were imposed for SOx emissions, which resulted in 545.72 kilo tonnes that are dispersed in the atmosphere annually according to this estimate [11].

These high values are also due to the way in which the vessels operating in the Black Sea are maintained, many of them being very old even with the operating period resulting from the design exceeded 2 times.

Other European studies [14,15] claim that emissions from ships in 2009 represent 19% of total NOx emissions, 12% of total SO2 emissions and 5.2% of PM10 total. These percentages vary, however, depending on the geographical situation and the proximity of the waterways and ports. The Romanian coastal area is in an unfavorable case due to the numerous ports that are in the region and the navigable routes to the Ukrainian ports that are 50-60 miles away from the Romanian shore, this specification characterizing the European navigable area where 89% of the emissions are produced at less than 50 miles from shore and 97% of cases at less than 100 miles from shore [14]. According to the study above mentioned (see Table 1 from [14]), in the area of the Mediterranean and the Black Sea the following values are assigned in 2009, at the same time an estimate was made for the year 2030 (see Table 3).

Table 3. Mediterranean and Black Sea emission 2009 and 2030

Mediterranean and Black Sea					
Year\Emissions (Ktonnes)	**Nox**	**SO2**	**CO**	**PM2.5**	**PM10**
2009	1701	1194	188	137	144
2030	1735	264	188	31	33

Referring to Table 3 and taking into account the trend of expansion of the global fleet, which brings with it a greater fuel consumption is supported only by the worldwide approach of strict regulations and in force to regulate the shipping activity for the purpose of shipping. reducing emissions as a result of fuel consumption. This expansion was met during the years 1950-2001, where we meet the following considerations [15]:

A considerable source of pollution in the coastal area is the fact that it is near numerous ports. For example, in Constanta port one of the largest ports in the Black Sea and in the top 20 in Europe [5] are issued in the atmosphere every hour according to a recent average estimate: between 2 and 2.5 tons of SOx, 1- 1.5 tons NOx and about 12 kg of PM10 [12].

All the above information, which results largely from calculations, following the application of a series of mathematical models and technical constraints, is confirmed by evaluations of the data collected with the help of satellite images, statuettes that have been equipped with equipment capable of performing tropospheric spectroscopy [16].

4. Conclusions

The present study is focused on the Black Sea basin and discusses the pollution-induced by the ships in this area. Commercial vessels use as fuel for diesel engines, few are LPG / LNG. Ships equipped with full electric transmission cannot be found in the Black Sea basin, because in general they are intended for relatively short distances such as access to islands, in case of ferries. Gasoline is used only for dealerships, which most often have a removable engine. The fact that freight activities by water have an influence on changing the concentrations that form atmospheric air is a reality. The air quality is based on an allowable concentration of substances, which must be found in a certain percentage of the general composition, and the way in which this economic activity influences the concentrations of component gaseous elements of the atmospheric air results that the activity itself influences the quality of the air in the areas bordering her area.

However, environmental factors do not yet favour the accumulation in the atmosphere of considerable quantities of polluting agents due to the active air currents in the coastal area that have a dispersing role. Also, the phenomenon of rain has the role of cleaning the air, a phenomenon quite common on the Romanian coast.

The coastal area is an area of interest for such studies due to the risk potential it presents both because of its proximity to sea routes to other locations (less than 60 miles) and the fact that ships arriving in ports reduce considerable speed, which is materialized by the increase of emissions such as NOx, and PM. The difference for PM can be more than 6 times higher, in case of reduced speeds compared to the cruise speed navigation situation [17,18].

A series of measures to combat these effects exist and can be taken into account:

(1) Use in ports of solutions such as those of shore-connection completed by LNG plant facilities in ports [13]. The SOx emissions would tend towards 0, and the CO2 and NOx emissions would decrease considerably in these conditions.

(2) Slow steaming

In the period of economic crisis 2009-2012 shipping as an industry sought to reduce its costs) the cost of fuel representing up to 50% [19]) was deliberately chosen to reduce the speed of the fleets, which led to a decrease and up to 30% of the emissions that this industry is responsible for. This fact is confirmed by the evaluation of the satellite data [15].

(3) Use of quality fuels (with a low percentage of Sulfur) / fuel switch.

This solution is beneficial for reducing the percentage

 DOI: https://doi.org/10.30564/jms.v2i1.1287

of SOx emissions but it is very costly, many shipowners avoid increasing their operating prices since so far, the cost of fuel represents up to 50% of the total. The second option is only a compromise solution, because the emissions of pollutants would be as far as 150-200 miles away, which in the long term still affects the environment, reducing only the short-term effects locally.

(4) Technical solutions to reduce emissions by filtration (Scrubber).

This approach presents several types of technologies, which seem to be a viable solution. In the long term, since it is a new solution, they are unknown in terms of long-term operation and maintenance costs.

Acknowledgments

This work was supported by the project "Excellence, performance and competitiveness in the Research, Development and Innovation activities at "Dunarea de Jos" University of Galati", acronym "EXPERT", financed by the Romanian Ministry of Research and Innovation in the framework of Programme 1—Development of the national research and development system, Sub-programme 1.2. Institutional Performance. Projects for financing excellence in Research, Development and Innovation, Contract no. 14PFE/17.10.2018.

References

[1] EU climate action (Accessed August 2019): https://ec.europa.eu/clima/citizens/eu_en

[2] EMSA (Accessed September 2019): http://emsa.europa.eu/main/air-pollution/greenhouse-gases.html

[3] IMO, Third IMO. Greenhouse Gas Study, Executive Summary and Final Report, London, 2014 (Accessed September 2019): http://www.imo.org/en/OurWork/Environment/PollutionPrevention/AirPollution/Pages/Default.aspx

[4] L. Rusu, A. Raileanu, F. Onea. A Comparative Analysis of the Wind and Wave Climate in the Black Sea Along the Shipping Routes, MDPI Water, 2018, 10: 924. DOI: 10.3390/w10070924

[5] Maritime transport statistics - short sea shipping of goods. (Accesed in September 2019): https://ec.europa.eu/eurostat/statistics explained/index.php/Maritime_transport_statistics__short_sea_ shipping_of_goods

[6] V. Eyring, H. W. Kohler, J. van Aardenne and A. Lauer. Emissions from international shipping: 1. The last 50 years, Journal of Geophysical Research, 2005, 110: D17305. DOI: 10.1029/2004JD005619

[7] V. Rata, L. Rusu. ASSESSING THE TRAFFIC RISK ALONG THE MAIN BLACK SEA MARITIME ROUTES, Proceeedings of ICCTE Belgrade 2018. ISBN: 978-86-916153-4-5

[8] Marinetraffic.com (Accesed in September 2019): http://marinetraffic.com

[9] Google Earth application.

[10] Air Quality, Air Quality Monitoring National Network, (Accesed in September 2019): http://calitateaer.ro

[11] V. Rata, C. Gasparotti, and L. Rusu. The Importance of the Reduction of Air Pollution In The Black Sea Basin, Mechanical Testing and Diagnosis, 2017 (VII), 2: 5-15. ISSN: 2247 – 9635

[12] V. Rata, L. Rusu. Air pollutant products resulting from port activity of ships in Constanta harbour, Proceeding of SGEM Albena 2019 Conference, 2019. DOI: 10.5593/sgem2019/4.1/S19.104

[13] V. Rata, A. Hobjila, and L. Rusu. LNG to Power in the Romanian port of Constanta, E3S Web of Conferences 103, 01007, ICACER 2019. DOI: org/10.1051/e3sconf/201910301007

[14] Impacts of Shipping on UK Air Quality, 2017. (Accesed in September 2019): https://uk-air.defra.gov.uk/assets/documents/reports/cat11/1708081025_170807_Shipping_Report.pdf)

[15] V. Eyring, H. W. Kohler, J. van Aardenne and A. Lauer. Emissions from international shipping: 1. The last 50 years, Journal Of Geophysical Research, 2005, 110: D17305. DOI: 10.1029/2004JD005619

[16] K. F. Boersma, G. C. M. Vinken and J. Tournadre. Ships going slow in reducing their NOx emissions: changes in 2005–2012 ship exhaust inferred from satellite measurements over Europe, Environmental Research Letters, 2015, 10(7). doi.org/10.1088/1748-9326/10/7/074007

[17] Ø. Endresen and E. Sørgard, J. K. Sundet, S. B. Dalsøren, I. S. A. Isaksen, and T. F. Berglen and G. Gravir. Emission from international sea transportation and environmental impact, Journal Of Geophysical Research, 2003, 08(D17): 4560. DOI: 10.1029/2002JD002898

[18] M. Viana, P. Hammingh, A. Colette. X. Querol, B. Degraeuwe, I. de Vlieger and J. Aardenne. Impact of maritime transport emissions on coastal air quality in Europe, Atmospheric Environment, 2014, 90: 96-105. doi.org/10.1016/j.atmosenv.2014.03.046

[19] The impact of international shipping on European air quality and climate forcing, European Environment Agency 2013. (Accesed in September 2019): https://www.eea.europa.eu/publications/the-impact-of-international-shipping/file

DOI: https://doi.org/10.30564/jms.v2i1.1287

BILINGUAL PUBLISHING CO.
Pioneer of Global Academics Since 1984

Journal of Marine Science
http://ojs.bilpublishing.com/index.php/jms

ARTICLE

Direct Energy Production From Hydrogen Sulfide in Black Sea Water - Electrochemical Study

V. Beschkov* **E. Razkazova-Velkova** **M. Martinov** **S. Stefanov**

Institute of Chemical Engineering, Bulgarian Academy of Sciences, Sofia 1113, Bulgaria

ARTICLE INFO

Article history
Received: 29 October 2019
Accepted: 20 November 2019
Published Online: 29 December 2019

Keywords:
Marine water
Hydrogen sulfide
Energy production
sulfide driven fuel cell

ABSTRACT

A sulfide driven fuel cell is proposed to clean the Black Sea with the simultaneous A sulfide driven fuel cell is proposed to clean the Black Sea with the simultaneous production of energy. The process is hopeful even at low sulfide concentrations, i.e.10 to 25 mg/l being close to the ones in the Black Sea water. The main problem for the practical application of this type of fuel cell are the low current and power densities. The measurement of the generated electric current compared to the sulfide depletion show that the most probable anode reaction is oxidation of sulfide to sulfate. It is evident that parasite competitive reactions oxidation of sulfide occurs in the anode compartment of the fuel cell. The pH measurements shows that the transfer of hydroxylic anions from the cathodic compartment to the anodic one across the separating membrane is not fast enough to compensate its drop in the anode compartment.

1. Introduction

The Black Sea waters contain enormous amounts of hydrogen sulfide. There are other water basins rich of hydrogen sulfide, which are typical for closed water area with non-sufficient renewal rate, like lakes, e.g. the Caspian Sea, the Baltic Sea, some fjords in the Norwegian coast, but the Black Sea is known as the richest one.

There are different explanations of this phenomenon. Some authors claim that the reason for hydrogen sulfide accumulation is the "Great Flood" in ancient times when the saline water from the Mediterranian Sea had penetrated through the Bosphorus straits into the Black Sea being a fresh water lake so far. The result had been the death of all living organisms therein. However, this hypothesis cannot explain the sustainable increase of the hydrogen sulfide content in case its amount had been constant throughout the centuries. Some other authors state that the reason is its penetration in the water through cracks at the seabed.

The most reliable explanation is that the almost closed Black Sea is permanently polluted by the big rivers, i.e. the Danube, Dnepr, Dniestre, Don. The organic pollutants swept to the sea are suitable substrate for the plankton, which consumes the oxygen in the surface water layers. Its growth leads to exhaustion of oxygen prompting the thiobacteria to use sulfate anions as terminal electron acceptor. As a result sulfate are reduced to sulfide, or hydrogen sulfide.

Its concentration grows along the sea depth.

Its presence in the Black Sea water becomes noticeable at depths below 150 meters, reaching about 20 g dm^{-3} at the sea bottom at 2300 m depth. The total amount of hydrogen sulfide in the Black Sea is estimated to 4,6 billion

**Corresponding Author:*
V. Beschkov,
Institute of Chemical Engineering, Bulgarian Academy of Sciences, Sofia 1113, Bulgaria;
Email: vbeschkov@yahoo.com

 DOI: https://doi.org/10.30564/jms.v2i1.1340

metric tons [1]. The energy equivalent of this amount is given in Table 1 below.

Table 1. Energy potential of hydrogen sulfide

Equivalent to	Tons of oil equivalent	Electricity, TWh
4,6 billion tons H_2S	2.6 billion	31000

Additional huge amounts are generated annually with energy equivalent estimated at least to 31TWh [2]. For a reference, the annual consumption of electrical energy in Bulgaria for the year 2015 was 37.8 TWh.

There are different proposals for applications of hydrogen sulfide in the Black Sea. The majority are focused on its splitting to obtain hydrogen and sulfur, either by thermal [3], plasma [4] or electrochemical methods [5,6]. There are two drawbacks of this approach – the required energy for hydrogen production is bigger than the produced one and next, the sulfur is obtained in a colloidal state which is not convenient for further recovery. There is a proposal for an electro-catalytic method for sulfide oxidation in aqueous media using solid electrolyte membrane [7].

There are some other efforts to use hydrogen sulfide in a fuel cell in gaseous phase [8] but elemental sulfur is the only product of oxidation which blocks the electrode surface. Although high current and power densities were attained, these fuel cells are not appropriate for treatment of aqueous solutions.

Sulfide Driven Fuel Cell

Our idea is directly to utilize hydrogen sulfide as an electric energy source reaching two simultaneous goals – environmental one as cleansing the sea water from sulfide and direct electricity production. The generated electromotive force in an especially constructed sulfide-driven fuel cell (SDFC) operates in aqueous media [9,10]. The method is based on the redox reaction of sulfide to sulfate. The energy content of hydrogen sulfide is given by the enthalpy of the following reaction:

$$S^{2-} + 2O_2 = SO_4^{2-} - \Delta H, -\Delta H = -788 \text{ KJ/mole}$$

The principle of SDFC is shown in Figure 1. Two options are possible: one, operating with proton exchange between the anode and cathode compartments, and another one –with exchange of hydroxylic anions, cf. Figure 1. The electrode reactions are as follows.

For the proton exchanging process:

Anode: $S^{2-} + 4H_2O - 8e^- = SO_4^{2-} + 8H^+$, $E_o = 0.149$ V

Cathode: $2O_2 + 8H^+ + 8e^- = 4H_2O$, $E_o = 1.229$ V,

And for the OH^- - exchange case:

Anode: $S_2^- + 6OH^- - 6e^- = SO_3^{2-} + 3H_2O$, $E_o = -0.61$ V

$SO_3^{2-} + 2OH^- - 2e^- = SO_4^{2-} + H_2O$

$E_o = -0.90$ V; Total: -0.706 V.

Cathode: $2O_2 + 4H_2O + 8e^- = 8OH^-$ $E_o = 0.401$ V

All standard potentials are calculated vs. the standard hydrogen electrode. The theoretical electromotive force of such a fuel cell element is 1.08 V.

The reaction enthalpy will be converted to electricity with high efficiency. This energy is "carbon-free" and it may drastically reduce the expenses for carbon quotas for the country-producer. According to theoretical calculation the Black Sea water with 20 g dm^{-3} with a flow rate 1 m^3/s yields 500 kW of electric power.

The principle of this type of fuel cell is shown in Figure 1.

The proposed process consists of the following steps:

(1) Pumping sea water from appropriate depth (e.g., 1000 m) to a rig on the sea surface where the equipment is installed;

(2) Enrichment to economically feasible concentration of hydrogen sulfide;

(3) Passing the enriched water through SDFC and generating electromotive force.

The treated water containing sulfate is taken off to the sea to appropriate depth where the sulfate anions serve as terminal electron acceptor for the thiobacteria there. Hence, new amounts of hydrogen sulfide are generated, ready for energy production, and so on. Therefore, in this case hydrogen sulfide could be considered as renewable carbon-free energy source.

The produced energy could be directly transmitted to the grid after DC/AC transformer or used directly for local applications, like feeding oil- or gas-extracting rigs with electricity or for hydrogen production after splitting water by electrolysis.

In the present proposed technology there are no harmful substances or chemicals to menace the life in the sea and the environmental balance. Moreover, the largest pollutant of the Black Sea, what hydrogen sulfide is, will be converted into the compatible sulfate ions together with the yield of pure, carbon-free energy from a renewable source. From this point of view the proposed method gives more environmental benefits (although modest as a scale) than harms.

The main important features of the proposed SDFC are:

Easy operation, easy switch on/off, carbon-free source of energy, renewable source (practically inexhaustible), no waste generation, environmentally compatible process.

The proposed method will be suitable for any water pond or mineral water spring where hydrogen sulfide is present. It could be applied for other wastewater streams containing sulfide. Restrictions could be imposed in de-

DOI: https://doi.org/10.30564/jms.v2i1.1340

pendence of the source capacity (total amounts and concentrations).

The advantages of the proposed technology from environmental and operational point of view to other energy sources are demonstrated in Table 2.

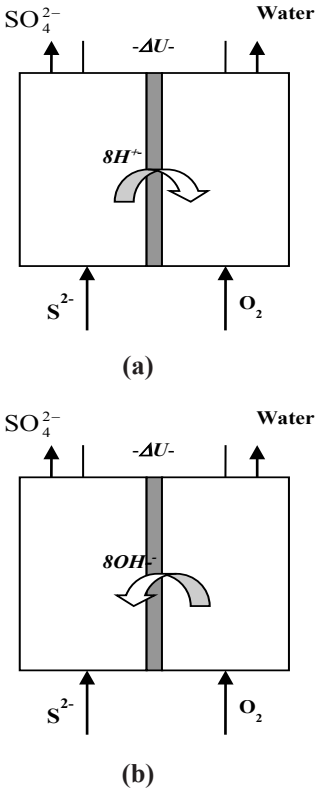

Figure 1. Principal sketch of sulfide driven fuel cell [11]. Proton (a) and OH^- (b) exchange across the membrane

Table 2. Comparison of features of sulfide driven fuel cell (SDFC) and other fuels

Energy source	Features	SDFC
Fossil fuels (oil, gas, coal)	Carbon emissions; expensive production; heavy operation; waste handling	Carbon free; less operational costs; easy switch-on/off; no waste
Nuclear fuel	Expensive fuel production; heavy operation; hazardous operation and waste storage	Less operational costs; easy switch-on/off; no waste; non-hazardous operations
Wind	Weather dependent; impact on environment	Independent; positive environmental impact
Solar	Weather dependent	Independent; positive environmental impact

The very technology and the technology conditions consist in the operations described above and the content of the sea water (i.e. sulfide and oxygen concentration, sulfate content, temperature, etc,). It could be expected, that higher sulfide concentrations will enhance the energy yield. However, pH of the water is dependent on the sulfide concentration because of the alkaline reaction of the sulfide solutions. The form of the sulfide ions are present depends strongly on the pH, cf. Figure 3. At higher sulfide concentrations reactions with polysulfide ions as a product are also possible. The latter are observed for pH values between 9 and 14. One can see that at pH within 7 – 9 hydrosulfide anions are predominant. This is the case in the Black Sea water.

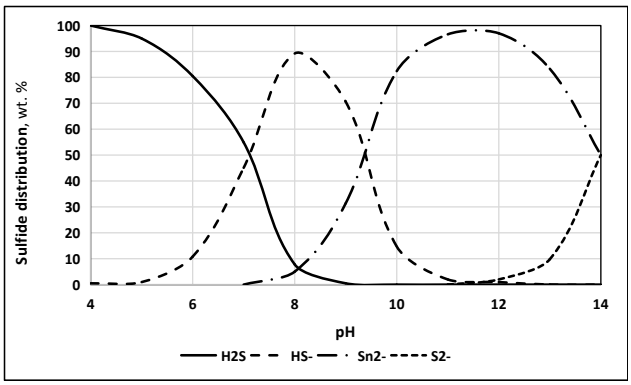

Figure 2. Distribution of different forms of sulfide ions depending on the pH value [12]

On the other hand, a large variety of sulfur oxidation reactions are possible. An excerpt of the list of such reactions is shown in Table 3. Both proton and hydroxide ion exchange processes are possible. The Gibbs free energies for some of the listed reactions involving different number of exchanged electrons are shown in the same table. Having in mind all these reactions one could expect that other oxidation reactions in the bulk could compete the electrochemical reactions on the fuel cell anode. The latter could be different depending on the reactions occurring in the bulk. Therefore the electricity yield may depend on the sulfide concentration (and the pH value), the oxygen concentration in the feeding solution and the anode reaction rate.

The Gibbs free energy ΔG for a certain electrochemical reaction can be calculated from the theoretical electromotive force E and the number of the exchanged electrons n by the equation:

$$\Delta G = -nFE, \quad (1)$$

where F = 96484.56 C mol^{-1} is the Faraday constant.

2. Aims

Depending on all these factors various situations are possible associated with different reactions (or combinations of them). That is why the energy yield could be quite different.

The aims of the present paper are:

(1) To study the anode electrochemical reactions of sulfide at different initial sulfide concentrations and

 DOI: https://doi.org/10.30564/jms.v2i1.1340

temperatures;

(2) To obtain the polarization curves of the sulfide driven fuel cell at different sulfide concentration;

(3) To study the energy yields from a sulfide driven fuel cell at different initial and inlet sulfide concentrations in batch and continuous process to find optimum conditions for electric energy production.

Table 3. Short excerpt of sulfide oxidation reactions, from [13]. Comparison of anode reactions and total reaction Gibbs free energies. An oxygen reduction is presumed as cathode reaction

Reversible redox anode reactions (short excerpt)	Number of exchanged electrons per atom sulfur	Standard electrode potential [V], 25°C	Gibbs free energy -Δ*G* [kJ/mole], 25°C
1. $S_2^{2-} + 2e = 2S^{2-}$	1	-0.524	169
2. $S + 2e = S^{2-}$	2	-0.48	209
3. $S + H^+ + 2e = HS^-$	2	-0.065	249
4. $SO_4^{2-} + H_2O + 2e = SO_3^{2-} + 2OH^-$	2	-0.90	251
5. $2SO_4^{2-} + 4H^+ + 2e = S_2O_6^{2-} + 2H_2O$	2	-0.22	279.7
6. $S_2O_3^{2-} + 6H^+ + 8e = 2S^{2-} + 3H_2O$	4	-0.006	476.4
7. $S_2O_3^{2-} + 8H^+ + 8e = 2HS^- + 3H_2O$	4	0,2	476.6
8. $SO_3^{2-} + 3H_2O + 6e = S^{2-} + 6OH^-$	6	-0.61	585
9. $SO_4^{2-} + 8H^+ + 8e = S^{2-} + 4H_2O$	8	0.149	833.3

3. Experimental: Materials and methods

3.1 Materials

Experiments without catalyst were carried out. The sulfide solutions were prepared by sodium sulfide nona-hydrate ACS reagent ≥.98% (Sigma-Aldrich production) or by sodium hydrosulfide, NaHS. As supporting electrolyte "sea salt" crystallized from Black Sea water or genuine sea water taken from depths below 200 up to 1000 meters were used. The salt concentration of the prepared solutions was close to the salinity of the natural Black Sea water, i.e.16 g dm^{-3}. The initial solution pH varied between 6.3 and 12.6 depending on the chosen sulfide concentration from 30 to 1000 mg dm^{-3}.

3.2 Methods

Experiments were carried in a lab-scale fuel cells designed for the present purpose (Fig 3a,b). The first one consisted of two co-centric cylindrical glass tubes separated by ion-exchange membrane with area of 7 cm^2 at the bottom of the inner vessel (Figure 3a). The latter was the cathodic space packed with granulated activated carbon particles (a Fujikasui production, Japan, S = 680 m^2g^{-1}) to increase the cathode surface. The volumes of the two spaces were 150 ml for the cathode space and 100 ml for the anodic one filled by sulfide solution. As electrodes cylindrical rods of spectral purity graphite were used. In some experiments as anode carbon felt was tested.

The second fuel cell was assembled as a stack of two cells, cf. Figure 3b. Each one consisted of two plane parallel rectangular graphite plates separated by the ion-exchange membrane (noted by dashed line). The electrodes were made out of sintered graphite plates (50 x 13 cm and 650 sq.cm area). The EDX-spectrum of the graphite plates showed contamination of silicon only.

In this case granulated activated carbon was also added to the cathode spaces. The slots between the electrodes and the membranes were 0.8 cm.

In both cases anion exchange membrane (Celgard 3501) was used. Air or pure oxygen was used as oxidant and it was blown in the cathode space. In another set of experiments the cathode electrolyte was previously aerated outside the fuel cell in a Venturi-tube ejector and circulated through the cathode compartments. The electrolyte in the cathode compartment was the same as the supporting one in the anode space.

The anode potential U_a was measured vs. saturated calomel electrode. The electromotive force of the cell $E = U_c - U_a$ and the current were measured during the experiments.

Both batch and continuous processes were studied. In the case of batch processes the agitation was accomplished by peristaltic pump. The same pump was used for feeding in the continuous experiments.

3.3 Analyses

Samples from the solution in the stirred reactor and the outlet solution were taken regularly. They were analyzed for sulfide, sulfite and sulfate ions together with the feeding solutions. The pH values of the feeding solutions and the outlet ones were measured by pH-meter. Sulfide was analyzed quantitatively by photometry [14]. Sulfite was analyzed iodometrically. Sulfate ions were analyzed turbidimetrically after addition of barium chloride (APHA). Formation of polysulfides was checked qualitatively by acidification of the reaction mixture and deposition of elemental sulfur. The presence of thiosulfates was checked qualitatively by ferric chloride yielding intensive purple complex.

3.4 Polarization Experiments

The polarization curves for the fuel cells were evaluated varying the current by external Ohmic resistance and measuring the corresponding cell voltage. Additionally

DOI: https://doi.org/10.30564/jms.v2i1.1340

the fuel cell power is calculated by multiplying the cell voltage by the electric current.

3.5 Cyclic Voltammetry

These experiments were carried out in the cylindrical fuel cell, Figure 4a. For maintenance of constant anode potential a potentiostat DECM (Hungary) was used. A saturated calomel electrode was used as a reference electrode. The cyclic voltammetry was carried out by very slow variation of the anode potential in order to avoid non-equilibrium states in the fuel cell. The anode potential, the total cell tension and the electric current were monitored simultaneously. The equilibrium anode potentials when the electric current was zero were estimated by the intercepts on the current axis in the VA-curves. Then the overpotentials $\eta = U_a - U_{eq}$ were calculated and plotted versus the measured electric current. From these curves the exchange currents i_o and the anodic and cathodic transfer coefficients α_a and α_c were estimated for each sulfide concentration and temperature using the generalized Butler-Volmer equation:

$$i = io\left[e^{\frac{aaF}{RT}\eta} - e^{\frac{-acF}{RT}\eta} \right] \quad (2)$$

3.6 Fuel Cell Discharging Experiments

These experiments were carried out both in a batch and continuous mode, cf. Figure 4. In the latter ones the sulfide solution was fed into the fuel cell (a single one or a stack) by peristaltic dosage pump. The generated electromotive force $E = E_1+E_2$ was discharged through an Ohmic resistance selected for each separate case.

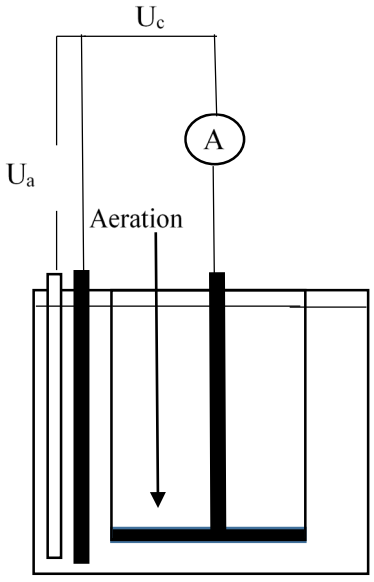

(a)

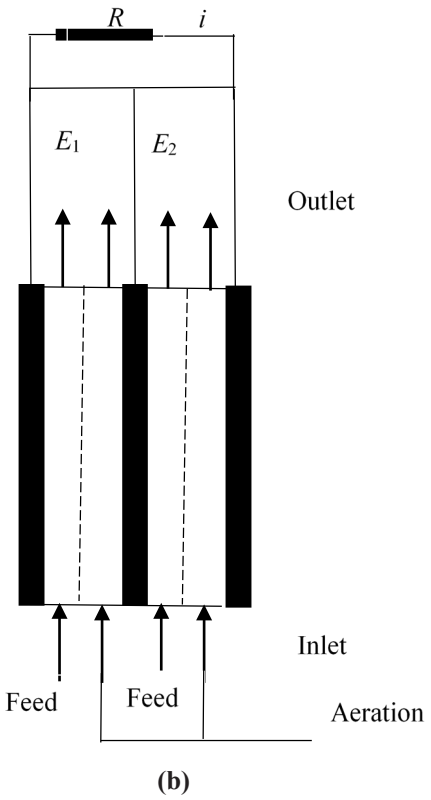

(b)

Figure 3. Sketches of the cylindrical fuel cell (a) and rectangular stack (b)

4. Results and Discussion

4.1 Cyclic Voltammetry

Some of the results obtained by cyclic voltammetry are shown in Figures 4-5. The first studied parameter and its influence is temperature, cf. Figure 4. It is seen that there is hysteresis in the V-A curves with area increasing with temperature. The equilibrium anode potentials (vs. the standard hydrogen electrode) when the net current is zero for the tested temperatures for the forward and reverse variation of anode potential corresponds to polysulfide formation from sulfide and hydrosulfide ions.

It means that there are irreversible reactions taking place at the anode.The higher the temperature, the bigger the hysteresis area. The highest anode potential corresponds to sulfide-to-sulfite and hydrosulfide-to sulfate-oxidation:

$$SO_3^{2-} + 6H^+ + 6e = S^{2-} + 3H_2O;\ E_0 = 0.233\ V/S.H.E.\ at\ 25^oC^-$$

and

$$SO_4^{2-} + 9H^+ + 8e = HS^- + 4H_2O.$$

 DOI: https://doi.org/10.30564/jms.v2i1.1340

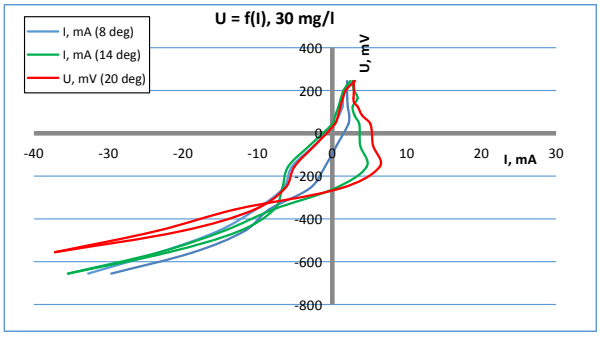

Figure 4. Voltammetry at different temperatures. Sulfide concentration, 30 mg/l

Since the experiments were carried out with sulfide as substrate and the pH was sufficiently high the first reaction is more probable.

The effect of initial sulfide concentration was tested for three different sulfide concentrations: 30, 60 and 120 g/l. The results for 120 g/l are shown in Figure 5. The hysteresis curves are more pronounced and more extended at the highest studied temperature (20°C). The equilibrium potentials have negative values, but still fit the conversion of sulfide to polysulfide.

Again, the maximum anode potential at 20°C corresponds to the sulfate formation at E_0 within 0.149 and 0.172 V/S.H.E.

Using the ButlerVolmer equation the transfer coefficients α_a and α_c were estimated for different temperatures. The anodic one α_a was about 0.14 and the cathodic one – around 0.1. The exchange current for both electrodes was about 0.1 mA in order of magnitude.

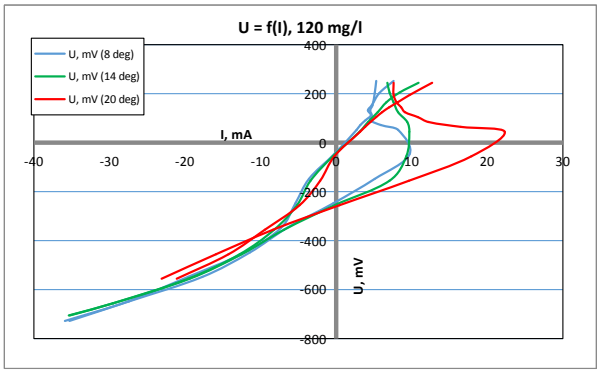

Figure 5. Voltammetry at different temperatures. Sulfide concentration, 120 mg/l

4.2 Polarization Curves

These curves were taken varying the external Ohmic resistance and plotting the cell voltage vs. the measured current. Experiments were carried out in one of the fuel cell of the rectangular stack. An example for experiment with genuine marine water at sulfide concentration of 25 mg/l is shown in Figure 6. This concentration was comparable with the maximum real concentration in the deep sea water. The initial pH value was 9.09, corresponding to considerable concentration of hydrosulfide, according to Figure 2.

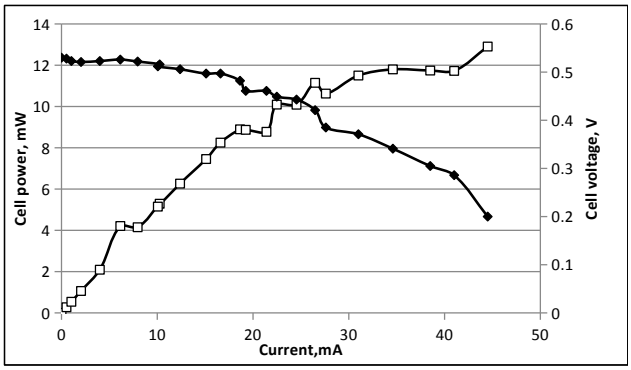

Figure 6. Polarization curve for stack of two fuel cells connected in parallel. (♦) – cell voltage; (□) - cell power. Sulfide concentration 25 mg/l; initial pH 9.09

The internal cell Ohmic resistance was estimated from the slope of the linear part of the voltage curve as 8 Ω. Certain over-potential of 17 mV was detected at very low electric current and some mass transfer resistance at the highest currents as well. It is a positive result that the open circuit potential in the case is 0.53 V, which is about 50% of the theoretical value for complete conversion of sulfide to sulfate. However, it is necessary to increase the current density [A cm^{-2}] and the power density [W cm^{-2}] to attain practically valuable results.

Polarization curves together with the calculated power for stacks connected in parallel and in series are shown in Figures 7 and 8 respectively. When the fuel cells were connected in parallel the open circuit potential was 0.68 V, i.e. this value is about 63% of the theoretical value. Note that the internal Ohmic resistance is rather low, i.e. about 1 Ω.

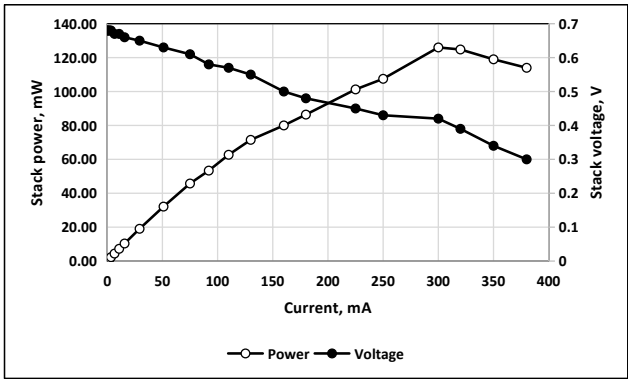

Figure 7. Polarization curve for initial sulfide concentration 240 g/l. Two fuel cells connected in parallel. (•) – stack voltage; (o) – stack power

The polarization curve for two cells connected in series is shown in Figure 8.

DOI: https://doi.org/10.30564/jms.v2i1.1340

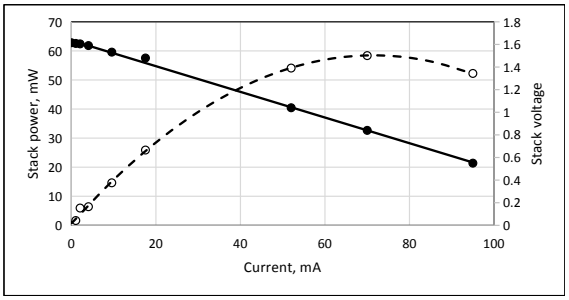

Figure 8. Polarization curve for initial sulfide concentration 236 g/l. Two fuel cells connected in series. (•) – stack voltage; (o) – stack power

In this case much higher voltage and open circuit are attained, i..e 1.6 V for OCP. However, the overall Ohmic resistance of the stack is higher, i.e. 11 Ω. That is why the measured current and the calculated power are lower than for the case of fuelcell connected in parallel.

4.3 Fuel Cell Discharge Experiments

These experiments were carried out by discharging the fuel cell (single or in a stack) through selected external Ohmic resistance in a continuous mode. Both parallel feed and consequent one into the stack was tested. Results for experiment with connected in series fuel cells are shown in Figure 9.

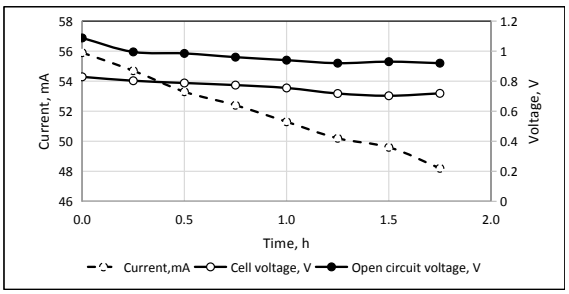

Figure 9. Fuel cell parameters for connected in series fuel cells in a continuous process. Feed sulfide concentration 250 mg/l. Feed flow rate 0.385 l/h

Results for connected in parallel fuel cells are shown in Figure 10. The comparison of the calculated current efficiency and the sulfide depletion according to the Faraday law and the results from the analysis shows that the most probable reaction is sulfite to sulfate anode oxidation, cf. Table 4.

Table 4. Comparison of the calculated and measured sulfide depletion with qualitative content of the inlet and outlet streams

	Calculated according to the Faraday law, mg/h	According to the analysis, mg/h	Qualitative content in the outlet stream	Fuel cell assembly
Figure 9	30.62	76.4	SO_3^{2-}; SO_4^{2}	In series
Figure 10	67.9	65.86	SO_3^{2-}; SO_4^{2-}	In parallel

The pH measurements show that there is a pH drop in the outlet streams, i.e. there is consumption of OH^- anions and reactions 4 and 8 from Table 3 take place. Obviously, oxidation of sulfide to sulfite occurs in the bulk as a parallel reaction competitive to the anodic one.

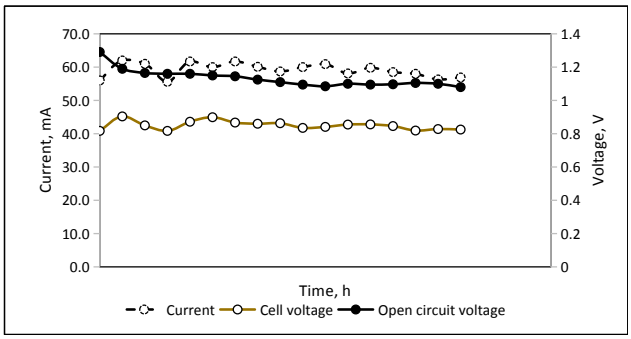

Figure 10. Fuel cell parameters for connected in parallel fuel cells in a continuous process. Feed sulfate concentration 270 mg/l. pH value in the feed 11.43

The pH drops in the solutes leaving the anode and cathode compartments shows, that the anion transfer across the separating membrane is the rate-controlling process.

The comparison in pH value drops for the anode and cathode compartments for a single experiment is shown in Table 5. The sulfide depletion is comparable to the pH drop in the anodic compartment. However, the pH increase in the cathode compartment is three order of magnitude lower and the transfer of hydroxylic anions across the membrane is retarded.

Table 5. Comparison in the pH variation in the inlet and outlet streams in the anode and cathode compartments. Sulfide concentration 70.5 g/l. Continuous flow, 220 ml/h feed flow rate.

Time,h	pH variation		OH^- change, g.eq.		Sulfide depletion, g.eq.10^4
	Anode compartment	Cathode compartment	Anode compartment	Cathode compartment	
1	-0.24	0.33	$-5.86.\ 10^{-4}$	$3.31.\ 10^{-7}$	$5.71.\ 10^{-4}$
2	-0.40	0.41	$-7.58.\ 10^{-4}$	$4.53.\ 10^{-7}$	$9.77.\ 10^{-4}$
3	-1.3	0.5	$-8.86.\ 10^{-4}$	$4.84.\ 10^{-7}$	$1.30.10^{-3}$
4	-0.60	0.5	$-7.49.\ 10^{-4}$	$4.84.\ 10^{-7}$	-
5	-0.80	0.59	$-7.48.\ 10^{-4}$	$6.62.\ 10^{-7}$	-

5. Conclusions

The experimental study leads us to the following conclusions.

(1) Sulfide anions can be used as a fuel for energy production in a newly designed fuel cell operating in aqueous phase. The process is hopeful even at low sulfide concentrations, i.e.10 to 25 mg/l being close to the ones in the Black Sea water.

DOI: https://doi.org/10.30564/jms.v2i1.1340

(2) The measurement of the generated electric current compared to the sulfide depletion show that the most probable anode reaction is oxidation of sulfide to sulfate, i.e. competitive oxidation of sulfide occurs in the bulk of the anode compartment of the fuel cell.

(3) The main problem for the practical application of this type of fuel cell are the low current and power densities.

(4) The pH measurements shows that the hydroxylic anions transfer from the cathodic compartment across the separating membrane is not fast enough to compensate its drop in the anode compartment.

These conclusions are helpful to outline measures to increase the fuel cell efficiency and to enhance the electrode reactions in order to attain practically interesting results.

Acknowledgement

This work was supported by the Fund for Scientific Research, Bulgaria, Grant E07/7 (2017).

References

[1] Midilli, A., Ay, M., Kale, A., Nejat Veziroglu, T. A parametric investigation of hydrogen energy potential based on H2S in Black Sea deep waters. Int. J. Hydrogen Energy, 2007, 32: 117– 124. DOI: 10.1016/j.ijhydene.2006.04.006

[2] Neklyudov, I.K., Bortz, B.V., Polevich, O.W., Tkachenko, V.I., Shilyaev, B.A. Alternative hydrogen sulfide energetics in the Black Sea. Part I. State of the art, problems and perspectives (in Russian). Int. Sci. J. Altern. Energy Ecol. (ISJAEE) 2006, 12: 23-30.

[3] Ouali, S., Chader, S., Belhamel, M., Benziada,M. The exploitation of hydrogen sulfide for hydrogen production in geothermal areas. Int. J. Hydrogen Energy, 2011, 36: 4103-4109. doi.org/10.1016/j.ijhydene.2010.07.121

[4] Linga Reddy, E., Biju, V.M., Challapalli, S.. Production of hydrogen and sulfur from hydrogen sulfide assisted by nonthermal plasma. Appl. Energy, 2012, 95: 87-92.

[5] Vasilevsky, V.V., Gutsevich, E.I., Rusanov, V.D. Problems of hydrogen sulfide and its treatment in the Black Sea (in Russian) Khim. Vys. Energ. 1995, 25: 382-386.

[6] Beschkov, V., Razkazova-Velkova, E. Utilization of sulphide from Black Sea water by electrolysis. Int. J. Current Chem. 2010, 1: 7-15.

[7] Ipsakis, D., Kraia ,T., Konsolakis, M., Marnellos, G.. Remediation of Black Sea ecosystem and pure H2 generation via H2S-H2O co-electrolysis in a proton-conducting membrane cell stack reactor: A feasibility study of the integrated and autonomous approach, Renew, Energy 2018, 806-818. DOI: 10.1016/j.renene.2018.03.005

[8] Chuang, K.T., Luo, J., Sanger, A.R.. Evolution of fuel cells powered by H2S-containing gases. Chem. Ind. Chem. Eng. Quart. 2008, 14: 69–76.

[9] Beschkov, V., Hristov, V., Petkov, P., Energy yield from sulfide containing marine water, BG Patent №1775/25.11.2013; ref. No. 2352/14.02.2013.

[10] Beschkov, V., Razkazova-Velkova, E., Vlaev, S.D., Martinov, M., Petkov, P., Raicheff, R., Method of oxidation of sulfide ions in fuel cells, BG Patent application, ref. No. 111367/17.12.2012.

[11] Beschkov, V., Razkazova-Velkova, E., Martinov, M.,Stefanov, S., Electricity Production from Marine Water by Sulfide-Driven Fuel Cell, Applied Sciences, 2018, 8(10): 1926; doi:10.3390/app8101926.

[12] Romero Cotrino, A., Control of hydrogen sulfide from groundwater using packed-bed anion exchange and other technologies, MSc Thesis, University of South Florida, USA, 2006: 8.

[13] Suhotin, A.M. (editor), Guidebook on electrochemistry (in Russian), Himia, Leningrad, 1981.

[14] Rees, T.D., Gyllenpetz, A.B., Dochery, A,C., Analyst, 1971, 96: 201.

DOI: https://doi.org/10.30564/jms.v2i1.1340

BILINGUAL PUBLISHING CO.
Pioneer of Global Academics Since 1984

Journal of Marine Science
http://ojs.bilpublishing.com/index.php/jms

ARTICLE

Characterization of Biofilm Forming Marine *Pseudoalteromonas spp*

Samia S. Abouelkheir[1*] Eman A. Abdelghany[2] Hanan A. Ghozlan[2] Soraya A. Sabry[2]

1. National Institute of Oceanography and Fisheries (NIOF), Marine Microbiology Lab., Kayet Bay, El-Anfushy, Alexandria, Egypt
2. Faculty of Science, Alexandria University, Egypt

ARTICLE INFO

Article history
Received: 5 November 2019
Accepted: 25 November 2019
Published Online: 29 December 2019

Keywords:
Biofilm
Pseudoalteromonas prydzensis alex
Pseudoalteromonas sp. Alex
Molecular identification
Marine rock
Marine sponge

ABSTRACT

Biofilm forming bacteria are omnipresent in the marine environment. *Pseudoalteromonas* is one of the largest within the γ-proteobacteria class, and a member of marine bacteria. Species of *Pseudoalteromonas* are generally found in association with marine eukaryotes. In this work, we present the isolation and characterization of two strains forming biofilm on rock surface and associated with marine sponge. They were identified using 16SrDNA as *Pseudoalteromonas prydzensis* alex, and *Pseudoalteromonas* sp. alex. They showed the highest titer in biofilm formation quantified using the test tube method using crystal violet.

1. Introduction

Bacterial biofilms form a highly structured community of cells attached to each other and/or a surface enclosed in a complex matrix of extracellular polymeric substances. These biofilms have several terms, including periphyton and mycrophytobenthos [1]. This phenomenon enables bacteria to colonize and prevalent in natural, industrial, and medical environments [2]. In marine environments, bacteria play important roles including driving biogeochemical cycles [3] and supplying materials and energy to higher trophic levels [4]. The phenotypic plasticity of bacteria is responsible for their success and ubiquity [5]. Biotic and abiotic surfaces in various marine environments are rapidly colonized by microorganisms, and surface colonization by marine microbes often involves biofilm formation [6]. Marine bacterial cells produce an extracellular polymeric substance (EPS) matrix after adhesions that establish the formation of a biofilm [1]. These biologically active compounds adapt bacteria to resist the extreme environmental conditions, such as high pressure, hydrothermal vent, and depletion of micronutrients [7].

The genus Pseudoalteromonas has attracted the attention of scientists because they are widely distributed in the marine environment and they are associated with a variety of marine organisms such as corals, sponges and others [8]. *Pseudoalteromonas* is a genus of Gammaproteobacteria that is widespread in the world's ocean and have been shown to produce bioactive compounds that inhibit settling of several fouling invertebrates and algae during biofilm formation [9].

It was thus aimed in this study to isolate, explore, and

**Corresponding Author:*
Samia S. Abouelkheir,
National Institute of Oceanography and Fisheries (NIOF), Marine Microbiology Lab., Kayet Bay, El-Anfushy, Alexandria, Egypt;
Email: samiaabouelkhir@yahoo.com

 DOI: https://doi.org/10.30564/jms.v2i1.1412

identify some marine biofilm forming bacteria attached to natural surfaces in sea water.

2. Materials & Methods

2.1 Bacterial Strains

The biofilm forming *Pseudoalteromonas prydzensis* alex, and *Pseudoalteromonas* sp. alex, were isolated from the surface rocks and sponge at Mediterranean seawater, Alexandria, Egypt. They were identified using 16SrDNA.

2.2 Media

Seawater (SW) medium was used for enrichment and isolation of biofilm forming bacteria. It contained (g/L): yeast extract, 1; peptone, 1; casamino acids, 1. Luria Bertani medium (LB) [10] composed of (g/L): tryptone, 10; yeast extract, 5; and NaCl, 10. Modified **Väätä**nen Nine Salts Solution (VNSS) [11] contained (g/l): NaCl, 17.6; $NaHCO_3$, 0.08; KBr, 0.04; $CaCl_2$. $2H_2O$, 0.41; $SrCl_2$. $6H_2O$, 0.008; Na_2SO_4, 1.47; KCl, 0.25; $MgCl_2$. $6H_2O$, 1.87; H_3BO_3, 0.008; $FeSO_4.7H_2O$, 0.01; Na_2HPO_4, 0.01; Peptone, 1.0; Starch, 0.5; Glucose, 0.5; Yeast extract, 0.5 that modified by replacing inorganic salts by seawater. Synthetic medium (SM) [12] had the following composition (g/L) NaCl, 24.53; $CaCl_2$. $2H_2O$, 1.54; KBr, 0.10; NaF, 0.003; KCl, 0.70; H_3BO_3, 0.03; Na_2SO_4, 4.09; $NaHCO_3$, 0.20; $SrCl_2$. $6H_2O$, 0.017; $MgCl_2$. H_2O, 11.1; KH_2PO_4, 1; K_2HPO_4, 1; $NaNO_3$, 1; NH_4Cl, 1; glycine, 1; glucose, 5; biotin, 5×10^{-8}, thiamine-HCl, 1×10^{-4}.

2.3 Bacterial Isolation

Biofilm forming bacteria were isolated by scrapping the surface of rock submerged in seawater and streaking on seawater agar plates. Sponge was cut into pieces in a flask containing seawater and shacked for 2h before streaking on SW agar plates and incubated at 30°C for 24h.

2.4 Biofilm Development in Glass Tubes

Biofilm formation technique was adopted by Hassan et al., (2011) [13]. Pure mucoid bacterial colonies showing different morphotypes were cultured onto SW agar plates for 48h then transferred into 5ml SW broth and left for another 48h under static condition at 30°C. The cells (OD_{600} of 0.15) were then harvested by centrifugation (6000x g, 5min) and re suspended in 5ml SW broth in test tubes to give a final volume of 5ml .Tubes were then incubated statically at 30°C for 24h to allow bacteria to form biofilms and used for biofilm assay . A negative control contained 5ml SW medium.

2.5 Biofilm Assessment

Quantification of cell adhesion and biofilm formation was performed by the method described by Haney et al., (2018) [14] based on staining biofilm with crystal violet (CV). The content of each tube was poured off after incubation and the attached bacterial cells were rinsed three times with 3ml phosphate buffer saline (PBS) prepared by dissolving NaCl, 8 g; KCl, 0.2 g; Na_2HPO_4, 1.44 g; and KH_2PO_4, 0.24 g in 800 ml distilled H_2O and pH adjusted to 7.4 with HCl then complete to a final volume of 1L and dried. Dried tubes with attached bacteria were fixed with 3ml of an aqueous crystal violet (CV) solution (1%) for 20min. Excess CV was removed and biofilms were rinsed with PBS. For quantification of biofilms, the attached stained cells were removed and re-suspended in 3ml ethanol (95%), and the absorbance was then measured spectrophotometrically at 600nm.

2.6 Genotypic Identification of ER9 and ER11

Genomic DNA was extracted from pure biofilm forming isolates according to Sambrook et al., (1989) [15]. The purity of the isolated DNA was confirmed by gel electrophoresis and subjected to polymerase chain reaction (PCR). The 16s rDNA was amplified using primers designed to amplify 1500 bp fragment of the 16s rDNA region. The forward primer was 5'AGAGTTTGATCMTGGCTCAG3' and the reverse primer was 5'TACGGYTACCTTGTTACGACTT3'. The PCR product was sequenced using the same PCR primers and confirmed by Gel electrophoresis according to Sambrook et al., (1989) [15]. The molecular phylogeny was performed using BioEdit software [16]. Sequences of rRNA genes, for comparison, were obtained from the NCBI database. The phylogenetic tree was displayed using the TREEVIEW program.

2.7 Phenotypic Characterization

Phenotypic characteristics were determined for the selected isolates according to the standard methods described by Ventosa et al., (1982) [17].

3. Results & Discussion

3.1 Selection of Biofilm Forming Marine Bacteria

Thirty mucoid colonies developed on SW agar plates were screened for biofilm formation and quantified using the CV quantification method. This method was reported to be the most convenient for analyzing biofilm formation [18]. The method depends on that CV binds to negatively charged molecules, including nucleic acids and acidic polysaccharides, and therefore serves as an overall measure of the whole biofilm. The values of biofilm in test tubes ranged from OD_{600} 0.5 to OD_{600} 3. These values are in good agreement with those reported by other investigators in natural environments [14]. The highest values (OD_{600}= 2.7and 2.6) were recorded for

DOI: https://doi.org/10.30564/jms.v2i1.1412

isolates ER11 & ER9, respectively (Figure1).

Bacteria were classified according to the scheme of Hassan et al., (2011) [13] as follows: non biofilm producer (0), less than or equal to ODc; weak biofilm producer (+), OD greater than ODc and less than or equal to 2×ODc; moderate biofilm producer (++), OD greater than 2×ODc and less than or equal to 4×ODc; strong biofilm producers (+++), OD greater than 4×ODc. This classification is based upon the cutoff OD (ODc) value which was defined as three standard deviations above the mean OD of the negative control. Based on obtained data, 40% of the isolates were non-biofilm producers, whereas a 30% were classified as weak, 16.6% as moderate and 13.3 % as strong biofilm forming bacteria.

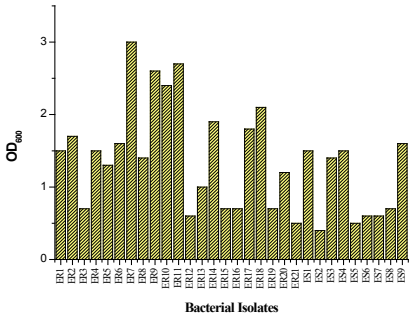

Figure 1. Quantification of biofilms formed by marine bacterial isolates grown in SW medium and incubated for 24h at 30°C

The distribution of biofilm forming bacteria on biotic and abiotic surfaces is depicted in Figure2. It is worth mentioning that the majority of biofilm forming bacteria (70%) were isolated from rock surface, whereas only 9 isolates (30%) were recovered from sponge. Biofilms cover most subtidal and intertidal solid surfaces such as rocks, ships, loops, marine animals and algae [19]. Surface roughness has been reported to be an important factor in bacterial attachment to inert surfaces. Other groups observed greater cell attachment on surfaces with high roughness [20]. In good agreement with our values, those reported by Bruhn et al., (2019) [21] for *Roseobacter* sp.

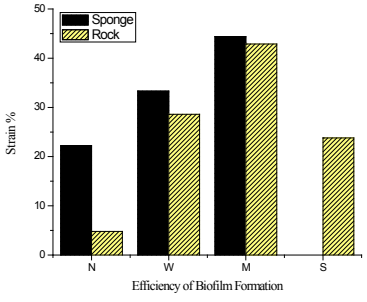

Figure 2. Percentage of biofilm forming bacteria isolated from sponge and marine rocks

Note: N= non biofilm formers; W= weak biofilm former; M= moderate biofilm former and S= strong biofilm former.

Data in Figure3a depict that according to scheme proposed by Hassan et al. (2011) [13], none of the isolates recovered from sponge were classified as strong producers, whereas, almost 44% were classified as moderate producers, 22% as normal producers and 33% as weak producers. The chart presented in Figure3b explains that the majority of isolates (42.9%) obtained from rock surface were moderate producers whereas, weak and strong producers represented 28.6 and 23.8% respectively.

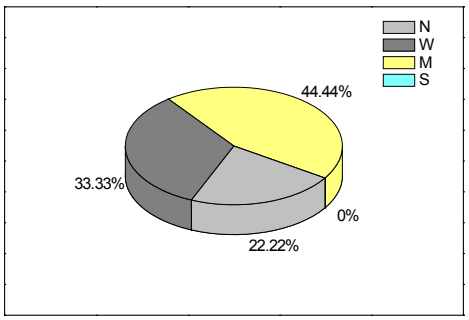

a

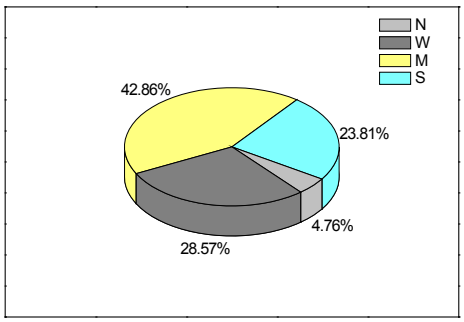

b

Figure 3. A chart showing the % of biofilm forming bacteria isolated from sponge (a) and a marine rock (b)

Note: N= non biofilm formers; W= weak biofilm former; M= moderate biofilm former and S= strong biofilm former.

3.2 The Role of Nutrient Status on Biofilm Formation

Indeed, attachment of bacteria to surfaces depends on the specific micro-niche created by marine particles [22]. Therefore, four media of different formulae (SW, LB, VNSS and SM) were used to select the best nutrient composition for biofilm formation. Data in Figure4 reveal that *In vitro* biofilm formation was highly dependent on medium composition. Synthetic medium (SM) did not support biofilm formation (data not shown) whereas, media containing natural compounds enhanced biofilm formation. In general SW medium containing low concentrations of natural substances (1 g of each of yeast extract, peptone and casamino acids) supported the *In vitro* biofilm formation as

indicated by the highest values of OD_{600} ranged from 1 to 3.0 compared to other tested media. Similarly, LB showed more or less compatible biofilm values to SW depending on bacterial strain. The suitability of seawater medium might be attributed to the low nutrient contents which support the growth and biofilm formation of oligotrophic marine bacteria. Oligotrophic environments are defined by low absolute concentrations of nutrients [23].

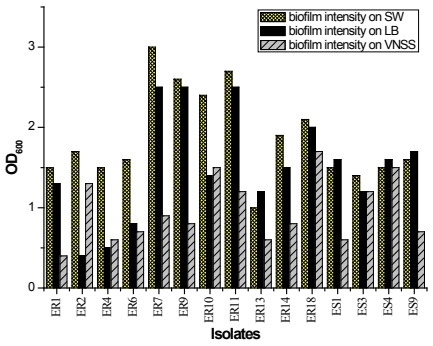

Figure 4. Values of OD_{600} as a measure of biofilm formation by marine isolates grown on different media

3.3 Microtitre Plate Versus Test Tube Method for Biofilm Formation

The microtitre plate was reported to be an easy, reliable and excellent method for screening a large number of isolates [24]. Therefore, this experiment was designed to compare the *In vitro* biofilm formation using the microtitre plate and test tube methods. From data shown in Figure5, it is concluded that under our experimental conditions the values obtained by the tube method were higher than those measured in microtitre plates. In some cases these values showed two or three fold increase compared to those of microtitre plates. Therefore, the tube method was adopted for further studies.

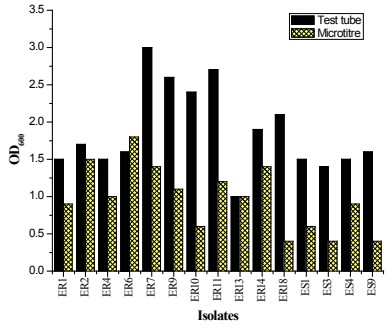

Figure 5. Quantification of biofilms formed by marine bacteria using Tube method versus Microtitre Plate

3.4 Phylogenetic Analysis of ER9 and ER11

The partial sequences of amplified 16SrDNA genes of ER9 and ER11 were aligned with closest relatives of sequences on database. Partial sequence of ER9 showed the highest homology (99%) to *Pseudoalteromonas* sp. OC-A5-12 and 98% to *Pseudoalteromonas prydzensis* strain CAIM381, whereas ER11 sequence analysis showed 97% similarity to several *Pseudoalteromonas* strains. Members of this genus have been most frequently isolated from marine biofilm, marine eukaryotes, seawater, sea ice, etc. [25, 8]. The two strains are members of Family *Pseudoalteromonadacea*, *Gammaproteobacteria*, and Phylum *Proteobacteria*. The sequences were deposited in GenBank with accession numbers JF965506 and JN592714 respectively. Members of *Gammaproteobacteria* have been reported to be one of the most abundant groups of readily cultivable heterotrophs from marine environment [26]. They possess a versatile pathway which explains their coexistence and survival in diverse environments [26]. Figures 6, 7 show the phylogenetic trees of the two isolates and their relation to other related species. Therefore, isolate ER9 was designated as *Pseudoalteromonas prydzensis* alex and ER11 was designated as *Pseudoalteromonas* sp. alex.

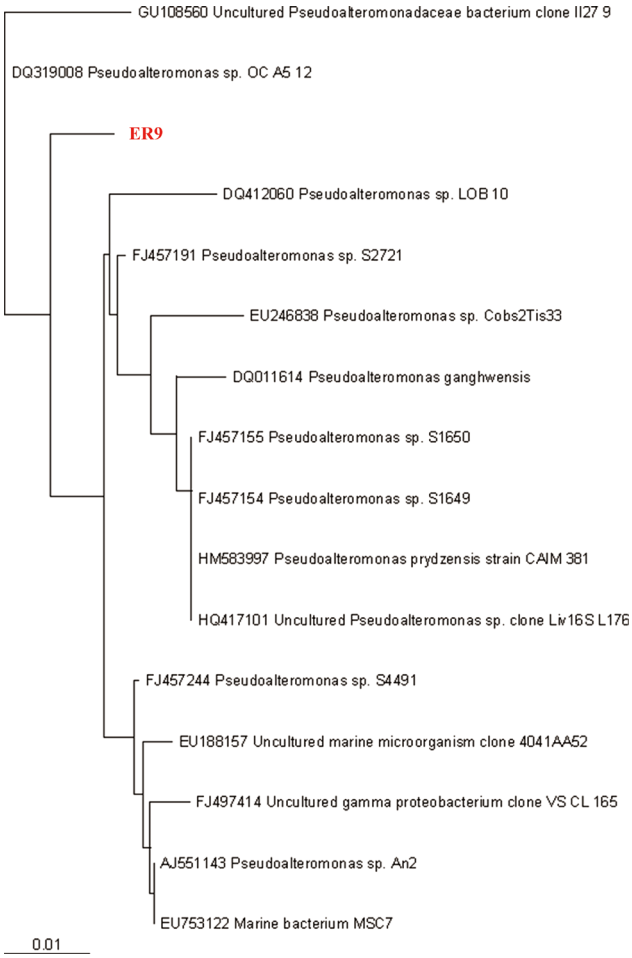

Figure 6. Phylogenetic tree of isolate ER9

Note: The dendogram based on partial 16S rDNA gene sequencing

DOI: https://doi.org/10.30564/jms.v2i1.1412

shows the phylogenetic position of the isolate among representatives of related bacterial species

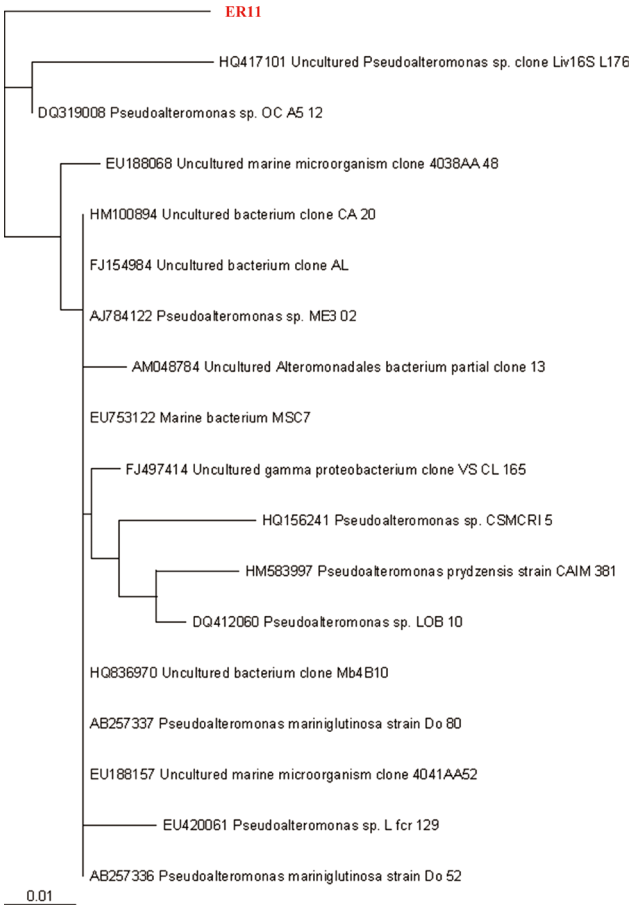

Figure 7. Phylogenetic tree of isolate ER11

Note: The dendogram based on partial 16S rDNA gene sequencing shows the phylogenetic position of the isolate among representatives of related bacterial species

3.5 Phenotypic Characterization

Phenotypic characterization of bacteria is complementary to phylogenetic data. Therefore, the two strains were subjected to some morphological, physiological and biochemical tests. Data are summarized in Table 1. It is worth mentioning that despite the difference in generic identification between the two *Pseudoalteromonas* strains, they both shared the same characteristic performed in this study.

Table 1. Differential characteristics of biofilm forming bacteria

Character	*P. prydzensis* alex	*P.* sp. alex
Colony morphology	Mucoid off-white	Mucoid off-white
Cell morphology	Short rods solitary	Short rods solitary
Gram stain	-	-
Metabolism		
Growth without sea water salts	-	-
Halotolerance (% NaCl)	10	10
Growth at:		
10°C	-	-
15°C	+	+
20°C	+	+
30°C	+	+
37°C	+	+
Biochemical		
Catalase	+	+
Oxidase	+	+
H_2S production	-	-
Nitrate reduction	-	-
Hydrolysis of		
Dextrin	+	+
Starch	+	+
Cellulose	-	-
Casein	+	+
Gelatine	-	-
Chitin	+	+
Tween 20	+	+
Tween 80	+	+
Oil	+	+
Utilization		
D-Glucose	-	-
D-Fructose	-	-
Maltose	+	+
Sucrose	-	-
Lactose	-	-
Galactose	-	-
Reaction to antibiotic		
Ofloxacin	R	R
Cefuroxime	S	S
Levofloxacin	R	R
Imipenem (Tinam)	S	S
Ampicillin/Sulbactam	S	S
Vancomycin	S	S
Augmentin	S	S
Ciprofloxacin	R	R
Amikacin	S	S
Ampicillin	S	S
Netilmicin	R	R
Meropenem	S	S
Cefotaxime	S	S
Chloramphnicol	R	R
Nitrofurantin	S	S
Norfloxacin	R	R

 DOI: https://doi.org/10.30564/jms.v2i1.1412

4. Conclusion

Marine microbes live attached to surfaces forming biofilms which are of significant importance from the biotechnological point of view. Two *Pseudoalteromonas* isolated from rock surfaces were the most potent in biofilm formation as detected by the tube method using crystal violet. This genus is very important in producing valuable molecules, thus further investigations are planned in the future.

References

[1] de Carvalho C.C.C.R.. Marine Biofilms: A Successful Microbial Strategy with Economic Implications. Front. Mar. Sci. 2018, 5: 126. DOI: 10.3389/fmars.2018.00126

[2] Tahrioui, A., Duchesne, R., Bouffartigues, E., Rodrigues, S., Maillot, O., Tortuel, D., Hardouin, J., Taupin, L., Groleau, M., Dufour, A., Déziel, E., Brenner-Weiss, G., Feuilloley, M., Orange, N., Lesouhaitier, O., Cornelis, P., & Chevalier, S.. Extracellular DNA release, quorum sensing, and PrrF1/ F2 small RNAs are key players in Pseudomonas aeruginosa tobramycin-enhanced biofilm formation. npj Biofilms and Microbiomes. 2019, 5(15): 1-10.

[3] Hawley, A.K., Nobu, M.K., Wright, J.J., Durno, W.E., Morgan-Lang, C., Sage, B., Schwientek, P., Swan, B.K., Rinke, C., Torres-Beltrán, M., Mewis, K., Liu, W., Stepanauskas, R., Woyke, T., & Hallam, S.J.. Diverse Marinimicrobia bacteria may mediate coupled biogeochemical cycles along eco-thermodynamic gradients. Nat. Commun, 2017, 8: 1507. DOI: 10.1038/s41467-017-01376-9

[4] de Carvalho, C.C.C.R., & Caramujo, M.J.. Lipids of prokaryotic origin at the base of marine food webs. Mar. Drugs. 2012, 10: 2698–2714. DOI: 10.3390/md10122698

[5] Brooks, A.N., Turkarslan, S., Beer, K.D., Lo, F.Y., & Baliga, N.S.. Adaptation of cells to new environments.Wiley Interdiscip. Rev. Syst. Biol. Med. 2011, 3: 544–561. DOI: 10.1002/wsbm.136

[6] Dang, H., & Lovell, C.R.. Microbial surface colonization and biofilm development in marine environments. Microbiol. Mol. Biol. Rev. 2016, 80: 91–138. DOI: 10.1128/MMBR.00037-15

[7] de Carvalho, C.C.C.R., & Fernandes, P.. Production of metabolites as bacterial responses to the marine environment. Mar. Drugs. 2010, 8: 705–727. DOI: 10.3390/md8030705

[8] Zeng, Z., Cai, X., Wang, P., Guo, Y., Liu, X., Li, B. & Wang, X.. Biofilm Formation and Heat Stress Induce Pyomelanin Production in Deep-Sea *Pseudoalteromonas* sp. SM9913. Front. Microbiol. 2017, 8: 1822. DOI: 10.3389/fmicb.2017.01822

[9] Ballestriero, F., Thomas, T., Burke, C., Egan, S., & Kjelleberg, S.. Identification of compounds with bioactivity against the nematode Caenorhabditis elegans by a screen based on the functional genomics of the marine bacterium *Pseudoalteromonas* tunicata D2. Appl. Environ. Microbiol. 2010, 76: 5710–5717. DOI: 10.1128/Aem.00695-10

[10] Williams, M.P.M., & Liao, M.. Luria Broth (LB) and Luria Agar (LA) Media and Their Uses Protocol. Amer. Soc. for Microbiol. 2016: 1-4.

[11] Penesyan, A., Breider, S., Schumann, P., Tindall, B.J., Egan, S., & Brinkhoff, T.. Epibacterium ulvae gen. nov., sp. nov., epibiotic bacteria isolated from the surface of a marine alga. Int. J Syst. Evol. Micr. 2013, 63: 1589–1596.

[12] Henson, M.W., Pitre, D.M., Weckhorst, J.L., Lanclos, V.C., Webber, A.T., & Thrash, J.C.. Artificial Seawater Media Facilitate Cultivating Members of the Microbial Majority from the Gulf of Mexico. MSphere. 2016, 1(2): e00028-16. DOI: 10.1128/mSphere.00028-16

[13] Hassan, A., Usman, J., Kaleem, F., Omair, M., Khalid, A., Iqbal, M.. Evaluation of different detection methods of biofilm formation in the clinical isolates. Braz. j. infect. dis. 2011, 15(4): 305-311.

[14] Haney, E.F., Trimble, M.J., Cheng, J.T., Vallé, Q., and Hancock, R.E.W.. Critical Assessment of Methods to Quantify Biofilm Growth and Evaluate Antibiofilm Activity of Host Defence Peptides. Biomolecules, 2018, 8(29): 1-22.

[15] Sambrook, J., Fritschi, E.F., & Maniatis, T.. Molecular cloning: a laboratory manual, Cold Spring Harbor Laboratory Press, New York, 1989.

[16] Hall, T.A.. BioEdit A User-Friendly Biological Sequence Alignment Editor and Analysis Program for Windows 95/98/NT. Nucleic Acids Symp. Ser. 1999, 41: 95-98.

[17] Ventosa, A., Quesada, E., Rodriguez-Valera, F., Ruiz-Berraquero, F., Ramos-Cormenzana, A. Numerical taxonomy of moderately halophilic Gram-negative rods. J. Gen. Micobiol. 1982, 128: 1959-1968.

[18] Simões, M.; Simões, L.C.; Vieira, M.J.. A review of current and emergent biofilm control strategies. LWT Food Sci. and Tech. 2010, 43: 573-583.

[19] Wahl, M., Goecke, F., Labes, A., Dobretsov, S., & Weinberger, F.. The Second Skin: Ecological Role of Epibiotic Biofilms on Marine Organisms. Front Microbiol. 2012, 3(292): 1-21.

[20] Cheng, Y., Feng, G., & Moraru, C.I.. Micro- and Nanotopography Sensitive Bacterial Attachment

DOI: https://doi.org/10.30564/jms.v2i1.1412

Mechanisms: A Review. Front Microbiol. 2019, 10(191): 1-17.

[21] Bruhn, J.B., Gram, L., Belas, R.. Production of Antibacterial Compounds and Biofilm Formation by Roseobacter Species Are Influenced by Culture Conditions. Appl. Environ. Microb. 2019, 73(2): 442-50.

[22] Fontanez, K.M., Eppley, J.M., Samo, T.J., Karl, D.M., & DeLong, E.F.. Microbial community structure and function on sinking particles in the North Pacific Subtropical Gyre. Front. Microbiol. 2015, 6: 469. DOI: 10.3389/fmicb.2015.00469

[23] Christaki, U., Wambeke, F.V., Dolan, J.. Nanoflagellates (mixotrophs, heterotrophs and autotrophs) in the oligotrophic eastern Mediterranean: standing stocks, bacterivory and relationships with bacterial production. Mar. Ecol. Prog. Ser., Inter Research, 1999, 181: 297-307. ff10.3354/meps181297ff. ffhal-01829920f.

[24] Kırmusaoğlu, S.. The Methods for Detection of Biofilm and Screening Antibiofilm Activity of Agents, 2019. DOI: http://dx.doi.org/10.5772/intechopen.84411.

[25] Beleneva, I.A., Skriptsova, A., Svetashevet, V.. Characterization of biofilm-forming marine bacteria and their effect on attachment and germination of algal spores. Microbiology, 2017, 86(3): 317-329.

[26] Franco, D.C., Signori, C.N., Duarte, R.T.D., Nakayama, C.R., Campos, L.S., & Pellizari, V.H.. High Prevalence of Gammaproteobacteria in the Sediments of Admiralty Bay and North Bransfield Basin, Northwestern Antarctic Peninsula. Front. Microbiol. 2017, 8: 153. DOI: 10.3389/fmicb.2017.00153

 DOI: https://doi.org/10.30564/jms.v2i1.1412

Author Guidelines

This document provides some guidelines to authors for submission in order to work towards a seamless submission process. While complete adherence to the following guidelines is not enforced, authors should note that following through with the guidelines will be helpful in expediting the copyediting and proofreading processes, and allow for improved readability during the review process.

Ⅰ. Format

- Program: Microsoft Word (preferred)
- Font: Times New Roman
- Size: 12
- Style: Normal
- Paragraph: Justified
- Required Documents

Ⅱ. Cover Letter

All articles should include a cover letter as a separate document.

The cover letter should include:

- Names and affiliation of author(s)

The corresponding author should be identified.

Eg. Department, University, Province/City/State, Postal Code, Country

- A brief description of the novelty and importance of the findings detailed in the paper

Declaration

v Conflict of Interest

Examples of conflicts of interest include (but are not limited to):

- Research grants
- Honoria
- Employment or consultation
- Project sponsors
- Author’s position on advisory boards or board of directors/management relationships
- Multiple affiliation
- Other financial relationships/support
- Informed Consent

This section confirms that written consent was obtained from all participants prior to the study.

- Ethical Approval

Eg. The paper received the ethical approval of XXX Ethics Committee.

- Trial Registration

Eg. Name of Trial Registry: Trial Registration Number

- Contributorship

The role(s) that each author undertook should be reflected in this section. This section affirms that each credited author has had a significant contribution to the article.

1. Main Manuscript
2. Reference List
3. Supplementary Data/Information

Supplementary figures, small tables, text etc.

As supplementary data/information is not copyedited/proofread, kindly ensure that the section is free from errors, and is presented clearly.

Ⅲ. Abstract

A general introduction to the research topic of the paper should be provided, along with a brief summary of its main results and implications. Kindly ensure the abstract is self-contained and remains readable to a wider audience. The abstract should also be kept to a maximum of 200 words.

Authors should also include 5-8 keywords after the abstract, separated by a semi-colon, avoiding the words already used in the title of the article.

Abstract and keywords should be reflected as font size 14.

Ⅳ. Title

The title should not exceed 50 words. Authors are encouraged to keep their titles succinct and relevant.

Titles should be reflected as font size 26, and in bold type.

Ⅳ. Section Headings

Section headings, sub-headings, and sub-subheadings should be differentiated by font size.

Section Headings: Font size 22, bold type

Sub-Headings: Font size 16, bold type

Sub-Subheadings: Font size 14, bold type

Main Manuscript Outline

Ⅴ. Introduction

The introduction should highlight the significance of the research conducted, in particular, in relation to current state of research in the field. A clear research objective should be conveyed within a single sentence.

Ⅵ. Methodology/Methods

In this section, the methods used to obtain the results in the paper should be clearly elucidated. This allows readers to be able to replicate the study in the future. Authors should ensure that any references made to other research or experiments should be clearly cited.

Ⅶ. Results

In this section, the results of experiments conducted should be detailed. The results should not be discussed at length in

this section. Alternatively, Results and Discussion can also be combined to a single section.

Ⅷ. Discussion

In this section, the results of the experiments conducted can be discussed in detail. Authors should discuss the direct and indirect implications of their findings, and also discuss if the results obtain reflect the current state of research in the field. Applications for the research should be discussed in this section. Suggestions for future research can also be discussed in this section.

Ⅸ. Conclusion

This section offers closure for the paper. An effective conclusion will need to sum up the principal findings of the papers, and its implications for further research.

Ⅹ. References

References should be included as a separate page from the main manuscript. For parts of the manuscript that have referenced a particular source, a superscript (ie. [x]) should be included next to the referenced text.

[x] refers to the allocated number of the source under the Reference List (eg. [1], [2], [3])

In the References section, the corresponding source should be referenced as:

[x] Author(s). Article Title [Publication Type]. Journal Name, Vol. No., Issue No.: Page numbers. (DOI number)

Ⅺ. Glossary of Publication Type

J = Journal/Magazine

M = Monograph/Book

C = (Article) Collection

D = Dissertation/Thesis

P = Patent

S = Standards

N = Newspapers

R = Reports

Kindly note that the order of appearance of the referenced source should follow its order of appearance in the main manuscript.

Graphs, Figures, Tables, and Equations

Graphs, figures and tables should be labelled closely below it and aligned to the center. Each data presentation type should be labelled as Graph, Figure, or Table, and its sequence should be in running order, separate from each other.

Equations should be aligned to the left, and numbered with in running order with its number in parenthesis (aligned right).

Ⅻ. Others

Conflicts of interest, acknowledgements, and publication ethics should also be declared in the final version of the manuscript. Instructions have been provided as its counterpart under Cover Letter.

About the Publisher

Bilingual Publishing Co. (BPC) is an international publisher of online, open access and scholarly peer-reviewed journals covering a wide range of academic disciplines including science, technology, medicine, engineering, education and social science. Reflecting the latest research from a broad sweep of subjects, our content is accessible world-wide——both in print and online.

BPC aims to provide an analytics as well as platform for information exchange and discussion that help organizations and professionals in advancing society for the betterment of mankind. BPC hopes to be indexed by well-known databases in order to expand its reach to the science community, and eventually grow to be a reputable publisher recognized by scholars and researchers around the world.

BPC adopts the Open Journal Systems, see on ojs.bilpublishing.com

Database Inclusion

Asia & Pacific Science Citation Index

Creative Commons

China National Knowledge Infrastructure

Google Scholar

Crossref

MyScienceWork

BILINGUAL
PUBLISHING CO.
Pioneer of Global Academics Since 1984

Tel:+65 65881289
E-mail:contact@bilpublishing.com
Website:www.bilpublishing.com